11B.

CO2

THE METEOROLOGICAL MAGAZINE

HER MAJESTY'S STATIONERY OFFICE

December 1987

Met.O.978 No. 1385 Vol. 116

METEOROLOGICAL OFFICE Met.O.978

THE METEOROLOGICAL MAGAZINE

No. 1385, December 1987, Vol. 116

551.583:551.588:551.510.4

Simulation of climate change due to increased atmospheric carbon dioxide

J.F.B. Mitchell
Meteorological Office, Bracknell

Summary

Increases in the atmospheric concentration of carbon dioxide and other trace gases are expected to produce changes in climate with potential economic and social consequences. The use of numerical models to determine the likely changes in climate is reviewed, with the emphasis on the physical mechanisms producing the simulated changes in climate. The problems of detecting climate change are discussed briefly.

1. Introduction

Atmospheric carbon dioxide (CO_2) is, to a first approximation, well mixed throughout the troposphere and lower stratosphere. Measurements made at Mauna Loa, Hawaii indicate that the concentration of atmospheric CO_2 has risen from 316 parts per million by volume (ppmv) in 1958 to 342 ppmv in 1985 (Fig. 1), and was probably about 300 ppmv at the turn of the century (see Oeschger and Stauffer (1986)). This change is attributed mainly to the increased emission from fossil fuels (Fig. 2). It has been estimated that the concentration of atmospheric CO_2 could exceed 600 ppmv by the end of the next century, but this estimate is subject to the uncertainties in forecasting the future use of fossil fuels, and predicting the response of the natural carbon cycle. These topics are considered further in a recent review by US Department of Energy (1985a) and references therein. A comprehensive assessment of the natural carbon cycle is given by International Council of Scientific Unions (1979).

The possibility that artificially produced CO_2 might affect climate was first considered by Callendar (1938). However it is only over the last 15 years that the advent of numerical models of climate and confirmation of the accelerating increase in observed CO_2 concentrations has stimulated widespread interest in 'the CO_2 problem' (see, for example, US Department of Energy (1985a,b,c,d) and International Council of Scientific Unions (1986)). The modelling of the climatic effects of CO_2 has been pioneered by Manabe and colleagues at the Geophysical Fluid Dynamics Laboratory (GFDL) in Princeton and much of that work has been reviewed recently (Manabe 1983).

Here the emphasis will be on the understanding of the physical mechanisms relevant to CO_2-induced climate change as the state of the art is not yet adequate to make detailed quantitative predictions of climate change. In doing so, reference has been made to typical results rather than trying to give a comprehensive review of numerical studies of the effect of increased CO_2 on climate. (A more detailed survey of recent work is given in Schlesinger and Mitchell (1987).)

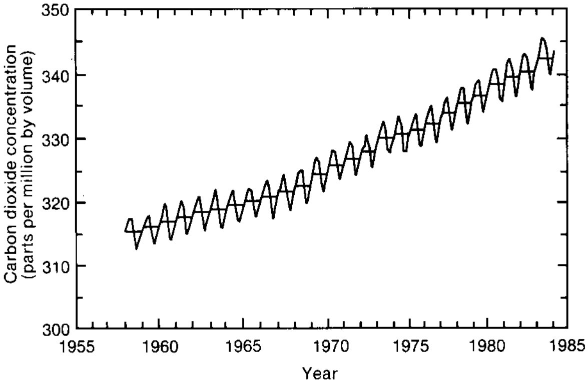

Figure 1. Concentration of atmospheric CO_2 at Mauna Loa Observatory, Hawaii. The horizontal bars represent annual averages and the diagram is reproduced from US Department of Energy (1985a).

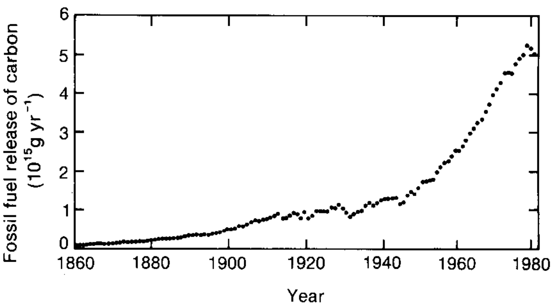

Figure 2. Fossil fuel emissions of carbon (from CO_2) from 1860 to 1982, from Marland and Rotty (1984) and reproduced in US Department of Energy (1985a).

The main concern will be with the effects of enhanced CO_2 from the beginning of the industrial revolution (about 100 years ago) until the end of the next century. In other words, we are interested in time-scales of up to a few centuries at most. We define a thermal response time to be the e-folding time to equilibrium (i.e. the time taken to reach 63% of the equilibrium temperature change due to a change in thermal forcing). As can be seen from Table I, the thermal response times of the atmosphere, land surface and upper ocean lie well within this time-scale, and that of the deep ocean partly so; hence these systems must be represented in our numerical models. On the other hand, the continental ice sheets have a much longer thermal response time, and hence it is assumed that, on the time-scale of interest, they will remain substantially unchanged.

Table I. *Thermal response times of various components of the climate system*

Component	Approximate response time (years)
Troposphere	0.05
Lower stratosphere	0.2–0.5
Land surface	0.2–1.0
Upper ocean	5–10
Deep ocean	100–1000
Continental ice sheets	≈ 10 000

2. Radiative forcing and simple feedback mechanisms

2.1 *Radiative effects*

The earth–atmosphere system is heated at a rate $(1-\alpha)S_0/4$ by solar (short-wave) radiation, where S_0 is the solar constant, α is the fraction of radiation reflected by the earth and atmosphere (currently about 0.33) and the factor of 4 allows for the spherical shape of the earth. This must be balanced by long-wave (thermal or infra-red) cooling to space. For a perfect emitter for example the earth's surface or thick cloud, the rate of long-wave cooling is given by σT^4, where T is the temperature of the emitter and σ is Stefan's constant. If the earth had no atmosphere, and α were unchanged, the surface temperature of the earth, T, would be given by

$$(1-\alpha)\,S_0/4 = \sigma T^4 \qquad \dots \dots \dots \dots \dots \dots \quad (1)$$

which gives an approximate value of T of 255 K (−18 °C). Certain gases (water vapour, carbon dioxide, ozone) absorb solar radiation weakly but strongly absorb and emit long-wave radiation. The (increased) downward long-wave radiation from these gases is responsible for the earth's surface temperature being 288 K (15 °C), some 33 K warmer than expected according to equation (1), a phenomenon often referred to as the 'greenhouse' effect.

Most of the radiation emitted to space emanates from the atmospheric gases rather than the surface. The effective emitting temperature of 255 K given by equation (1) corresponds to a height of about 6 kilometres. By increasing the concentration of an atmospheric absorber such as CO_2, the mean level from which radiation escapes to space moves to a higher, and therefore colder, level (see Fig. 3). The long-wave cooling to space is reduced and the earth–atmosphere system warms until the long-wave cooling again balances the incoming solar radiation.

The global mean temperature in the stratosphere is close to radiative equilibrium, but this is not true in the troposphere. If the temperature in the troposphere was controlled by radiation alone, the decrease in temperature with height (or lapse rate) would be much greater than observed (Manabe and Wetherald 1967). In regions where dense air overlies less dense air, the atmosphere produces overturning (mixing in the vertical, or convection) until the lapse rate is reduced to the stable value, which is 9.8 K km^{-1} for dry air. If moisture is present, rising air may cool sufficiently to become supersaturated, so that condensation occurs and latent heat is released. This further reduces the lapse rate, so the global mean value is about 6.5 K km^{-1}. To summarize, the equilibrium temperature of the troposphere is dependent on the balance between radiative cooling to space and the convective transfer of heat from the surface. Conversely, the surface is heated radiatively, and cooled by the loss of sensible and latent heat to the atmosphere. Both these processes must be represented in any model which is to be used to study the surface and tropospheric response to increased CO_2.

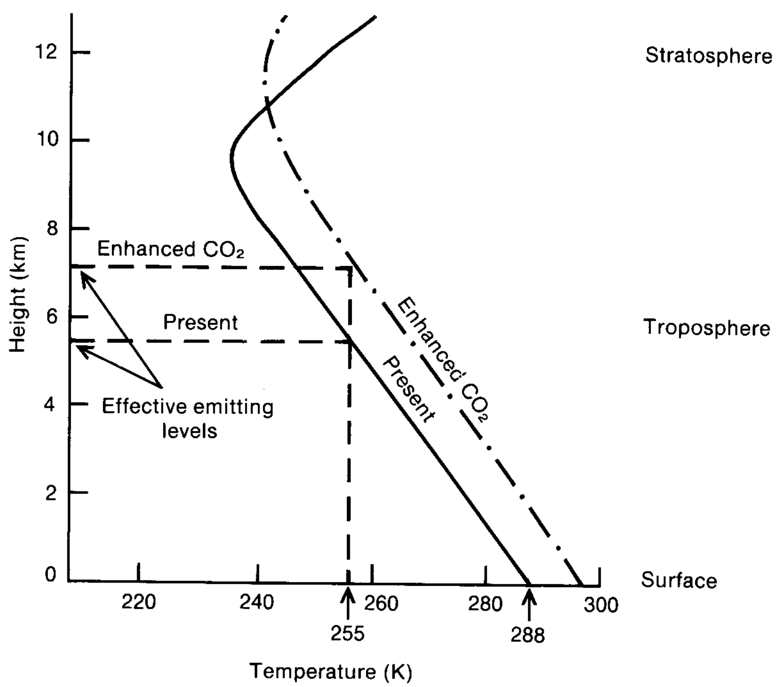

Figure 3. The effect of increasing CO_2 on the vertical profile of temperature (schematic representation).

2.2 *Some climate feedbacks*

Any model used to investigate the effect of increased CO_2 on the climate must be able to represent the important climate feedbacks; these are due to water vapour, sea-ice/snow, cloud cover and cloud optical properties.

(i) *Water vapour.* Increasing temperature by 1 K from 288 K increases the saturation vapour pressure of water by about 7%. Thus, it is to be expected that the atmospheric water vapour content will increase with temperature. Manabe and Wetherald (1967), on the basis of the observed seasonal variation of atmospheric humidity, concluded that relative humidity (the percentage of saturation) was approximately constant. This being the case, an increase in atmospheric temperature will be accompanied by an enhancement of atmospheric water vapour which increases the opacity of the atmosphere to long-wave radiation and thus enhances the warming of the atmosphere and earth's surface.

(ii) *Sea-ice/snow.* An increase in atmospheric temperature will tend to reduce highly reflective snow and sea-ice cover, leading to increased absorption of insolation and further warming. Clearly, the strength of this feedback will depend on the areal cover of snow and sea-ice, and hence the temperature of the unperturbed simulation. In general, the colder the simulation the greater the sensitivity of the model. Removal of sea-ice greatly increases the thermal inertia of the surface and reduces the amplitude of the annual cycle — this will enhance a warming in winter and reduce it in summer.

(iii) *Cloud-cover.* Clouds reflect solar radiation and absorb and emit infra-red radiation. A decrease in cloud cover reduces both the reflection of solar radiation, producing a surface warming, and the emission of long-wave radiation, producing a cooling. Current evidence suggests that the former effect is dominant at most latitudes where insolation is significant. The long-wave effects may be more important for high, thin cirrus. In addition, an increase in cloud height will also tend to warm the surface because radiation from the cloud top is emitted to space at a lower temperature.

Simulations with increased CO_2 using three-dimensional climate models show a consistent decrease in middle- and upper-tropospheric cloud at most latitudes, with increases in cloud in the lower stratosphere, particularly in middle and high latitudes (Schlesinger and Mitchell 1987). Similar changes have been found in an experiment using a version of the Meteorological Office 11-layer model in which CO_2 amounts were doubled (Wilson and Mitchell 1987b). These changes are consistent with an increase in the height of the tropopause. The observed tropopause is highest in low latitudes and in summer when insolation is strongest; thus there is at least circumstantial observational evidence that the model's response to tropospheric warming is physically correct.

The details of the above changes are obviously sensitive to the parametrization of radiation, particularly with respect to water vapour, and the vertical transport of water. The vertical resolution of most models is poor near the tropopause (generally there are three layers above 250 mb though the Meteorological Office model has four) and the vertical extent of cloud is usually limited; for example, in the Meteorological Office model used here it is confined below 60 mb.

(iv) *Cloud optical properties.* The parametrization of cloud has to date been based on relative humidity, although attempts have been made to devise a parametrization of cloud liquid water. This approach has the advantage that cloud optical properties can be related in a consistent manner to the liquid water content but, as yet, such liquid-water content parametrizations are fairly arbitrary. A general increase in atmospheric specific humidity might be expected to lead to an increase in cloud liquid-water content and hence the reflectivity of cloud. Stephens (1978) has derived simple parametrizations of the relation between cloud optical properties and cloud liquid-water content, based on observational data. He found a gradual increase in cloud reflectivity (albedo) with cloud liquid-water content, although the long-wave emissivity of thin cloud (e.g. cirrus) may also increase significantly. An increase in albedo would cool the surface; an increase in the long-wave emissivity of high cloud would have the opposite effect. It is by no means clear how one can relate cloud liquid-water content to large-scale model variables (e.g. temperature, humidity, etc.). Nevertheless, Somerville and Remer (1984) have attempted to do this by relating cloud liquid-water content to temperature, and find that the resulting negative feedback is sufficient to counteract all the positive feedbacks described earlier. In view of the uncertainties in their parametrization, the magnitude of cloud optical feedback is also extremely uncertain, and is a priority for future research.

3. Equilibrium studies using general circulation models

3.1 *Introduction*

Some aspects of climate change can be investigated economically using inexpensive one-dimensional models (for example, the initial study of water-vapour feedback made by Manabe and Wetherald (1967)). However, many factors such as horizontal transport, land–sea contrasts and the effects of orography are treated inadequately or omitted altogether. Furthermore, one-dimensional models cannot provide the regional variations which are needed to assess the possible impacts of climate changes, so there has been an enormous effort to develop and use the considerably more expensive three-dimensional models of climate.

The atmospheric component of a three-dimensional climate model can be regarded as a numerical prediction model which has been designed for long integrations. (Most of the physical parametrizations in the Meteorological Office forecast model have been taken from the Office's climate model with only minor modifications.) However, although general circulation models simulate the passage of individual disturbances, it is the behaviour of the model over long periods which is of interest. The philosophy for carrying out model 'experiments' is as follows. Firstly, the model is run for a long period, usually between several years and several decades, with present-day boundary conditions (in this case, present CO_2 concentrations). The length of simulation is chosen so that the long-term statistics (for example, monthly mean surface temperatures and inter-annual variances) are well defined and independent of the initial conditions. Then an anomaly simulation with enhanced CO_2 is made, and the difference in the statistics of the two simulations is examined to assess the impact of the changes.

As noted in section 1, atmospheric CO_2 and trace gases are increasing on a time-scale of decades to centuries, and hence changes in ocean temperatures and sea-ice must be taken into account. Due to the large thermal inertia of the deep oceans, it has not been practical to integrate a detailed climate model with a deep ocean to equilibrium, though this is now possible if the seasonal cycle of solar radiation is ignored. Hence, most work to date has involved models with grossly simplified representations of the ocean.

3.2 *An early study*

In the earliest study (Manabe and Wetherald 1975), oceanic heat storage and transport were ignored, and sea surface temperatures were determined diagnostically such that the net heat flux across the air–sea interface was zero. Sea-ice was predicted where the ocean temperature fell below the freezing-point of sea water. This representation of the ocean is often referred to as as 'swamp' ocean. The diurnal and seasonal variation of incoming solar radiation must be ignored in view of the neglect of the ocean's heat capacity. Manabe and Wetherald also limited the computational domain to a sector covering approximately one-sixth of the globe, used an idealized land–sea distribution and ignored the effects of topography.

The simulated equilibrium change in atmospheric temperature due to doubling CO_2 (Fig. 4) varies considerably with latitude. In low latitudes, the warming is about 2 K near the surface and increases to over 3 K at upper levels of the troposphere. As noted earlier, in the tropical atmosphere the vertical gradient of temperature tends to the moist adiabatic lapse rate which becomes smaller as temperature increases, leading to enhanced warming at upper levels. Conversely, in high latitudes, the surface warming is enhanced because the inherent stable stratification inhibits the transfer of heat to upper levels. Two further mechanisms contribute to the enhanced surface warming in high latitudes. Firstly, the increase in temperature will reduce the extent of highly reflective snow and sea-ice cover, leading to increased absorption of insolation and further warming (temperature–albedo feedback). Secondly, the atmospheric water content is greater in the warmer atmosphere, leading to a larger poleward transport of moisture and enhanced latent heat release in high latitudes. The areal mean warming on doubling CO_2 is 2.9 K.

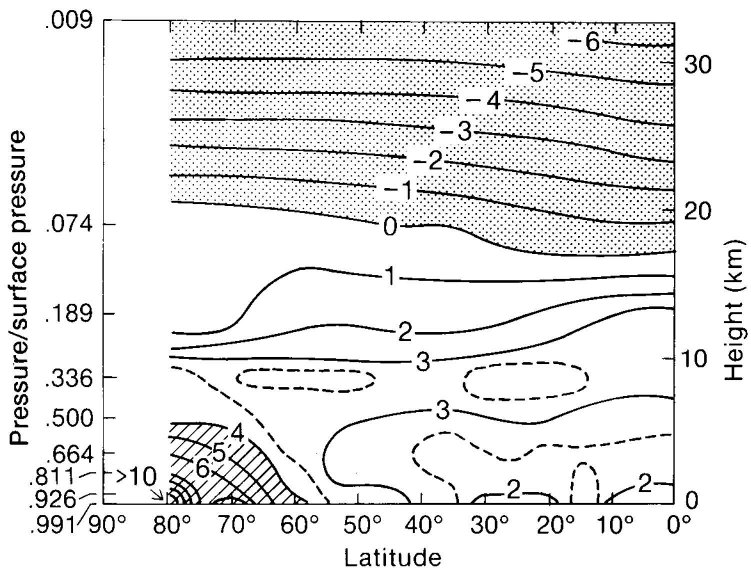

Figure 4. Height–latitude diagram of zonally averaged temperature changes (K) due to doubling CO_2 in an idealized climate model, from Manabe and Wetherald (1975). Changes greater than 4 K are shaded and less than zero stippled.

3.3 *A detailed study with prescribed cloud cover*

Useful as Manabe and Wetherald's study is for illustrating some of the physical mechanisms which contribute to changes in climate, it gives no guidance on the seasonal and regional changes which, for example, are necessary for the assessment of the likely social and economic effects of increased CO_2. To do so, one must use a model which includes the annual cycle of insolation. This has been attempted using two differing but complementary approaches.

In the first approach, the ocean is represented by a static pool with the depth (typically 50–70 metres) chosen to provide reasonable simulation of the annual cycle of sea surface temperatures over most of the oceans. A simple representation of sea-ice is also included. This approach allows the sea surface temperatures and sea-ice extents to interact with the atmosphere as it responds to the increase in CO_2 concentrations. It has the disadvantage that errors in the atmospheric model, and the crudeness of the ocean model, lead to errors in the simulation of present-day climate which may distort the response of the model to small perturbations.

Manabe and Stouffer (1980) investigated the effect of quadrupling CO_2 amounts in such a model with realistic geography and orography, and using prescribed zonally averaged cloud cover. The global mean surface temperature increased by 4.1 K. In the tropics, the warming is less than 3 K near the surface (Fig. 5) and increases to over 4 K in the upper troposphere, whereas in high latitudes in winter, especially over the Arctic, the warming is a maximum near the surface and decreases rapidly with height, in qualitative agreement with Manabe and Wetherald (1975). However, in high latitudes in summer, the lower atmosphere is not inherently stable in the unperturbed integration, and so the warming is more uniformly distributed in the troposphere. In the Arctic in summer, the near-surface warming is small for reasons discussed below.

In the 4 $\times$ CO_2 integration, the areal extent of highly reflective sea-ice is substantially reduced leading to enhanced absorption of solar radiation by the high-latitude oceans, particularly in summer (sea-ice

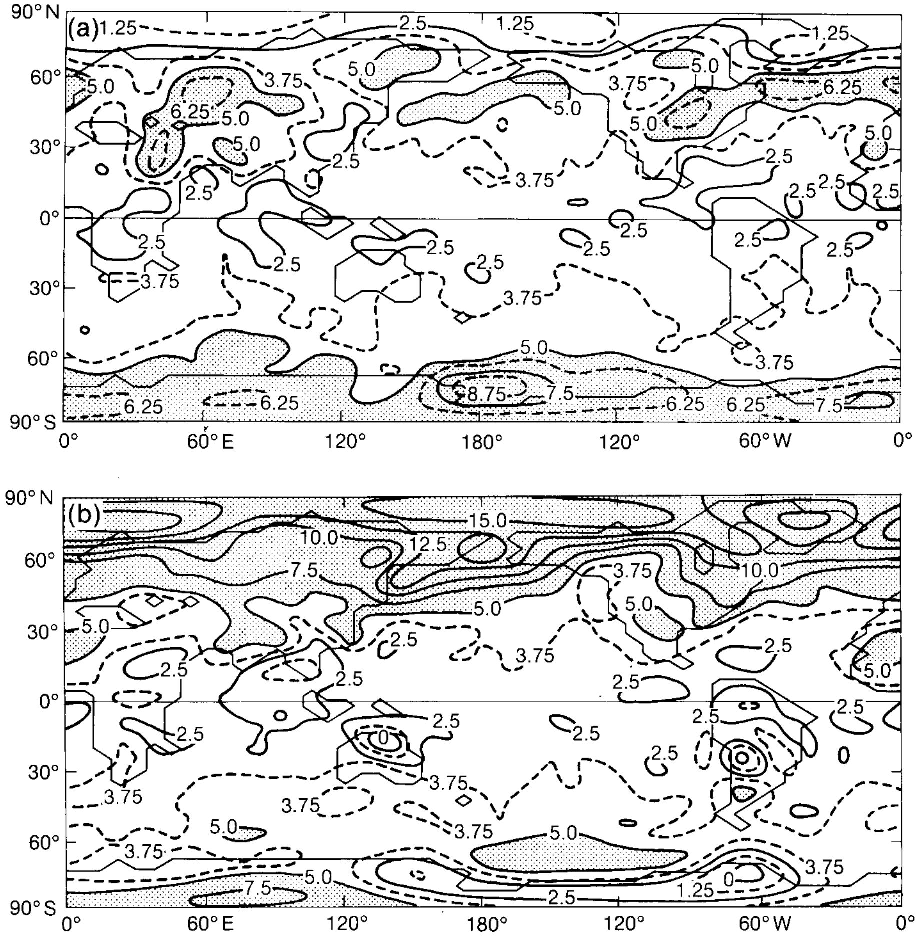

Figure 5. Average changes in surface air temperature (K) due to quadrupling CO_2 in a low-resolution climate model with prescribed cloud (Manabe and Stouffer 1980) from (a) June to August and (b) December to February. The areas with changes greater than 5 K are stippled.

disappears from the Arctic in summer and is absent from the Antarctic during most of the year). The enhanced ocean heat storage delays the formation of ice in autumn, leading to thinner ice in winter and consequently earlier melting of ice in spring. In the Arctic, the delay in the formation of sea-ice and the consequent reduction in the insulation of the atmosphere from the relatively warm mixed-layer surface leads to a maximum warming in autumn. In winter, there is still a substantial increase in surface air temperature since the atmosphere is inherently stable and the warming is confined to the lowest model layer as found by Manabe and Wetherald (1975). In summer, however, the warming is a minimum, despite increases of up 50 W m^{-2} in solar heating, because the large thermal inertia of the mixed layer prevents temperatures rising much above 271 K, the melting point of sea-ice. Around Antarctica, the seasonal variation in the temperature change is smaller, probably because the seasonal variation in the control integration is smaller than in the Arctic. The mean warming is also smaller, perhaps because the sea-ice in the control integration is thinner and less extensive than in the northern hemisphere (and less than the observed thicknesses).

Temperature changes over the northern hemisphere continents are generally similar to those over neighbouring oceans. In April, there is a secondary maximum warming near 60° N associated with the earlier removal of highly reflective snow cover in the $4 \times CO_2$ integration. Over Antarctica, the temperature–albedo feedback is much weaker, as throughout the year in the control integration the surface temperatures are substantially lower than the threshold above which albedo varies. This is largely a result of the height of the Antarctic plateau.

It should be noted that Manabe and Stouffer used a low-resolution (15 spectral waves) model which is inadequate to represent the weak baroclinic disturbances which are characteristic of the northern hemisphere mid-latitude summer circulation, and which on the western side of continents are associated with much of the summer precipitation. Furthermore, the neglect of the oceanic circulation leads to errors in the distribution of sea surface temperatures and sea-ice, which may distort the response of their model to enhanced CO_2. The errors in the sea-ice distribution in Manabe and Stouffer's control integration have already been noted. Even where atmospheric models have been coupled to a dynamical model of the ocean (Manabe *et al.* 1979, Washington *et al.* 1980, Gates *et al.* 1985) there are substantial errors in the simulated sea surface temperatures and sea-ice extents. Hence, some studies carried out in the Meteorological Office have followed a different strategy, which will now be described.

3.4 *Studies with prescribed cloud cover carried out at the Meteorological Office*

In the control integration used by the Meteorological Office, sea surface temperatures are prescribed from climatology. Since the changes due to CO_2 are sufficiently small to be regarded as a perturbation, the changes in sea surface temperature are prescribed on the basis of a succession of perturbation experiments which approximate equilibrium with increasing accuracy. The advantages of this approach are that the simulated control climate is not distorted by errors in sea surface temperatures and sea-ice, and the simulations attain equilibrium after about 1 year as opposed to 10 or more years needed with a 'slab' ocean. In the Meteorological Office, the consequent saving in computer time has allowed the use of high-resolution atmospheric models which are capable of representing baroclinic disturbances throughout the year. The disadvantage of the method is that the prescribed changes (particularly of sea-ice extent) are only approximately in equilibrium, and hence may influence other aspects of the model's response.

In the first Meteorological Office study (Mitchell 1983) the response of the ocean was ignored. In the second, also described by Mitchell (1983), the ocean temperature increase was assumed to be the same everywhere. In the third (Mitchell and Lupton 1984), the ocean temperature changes were prescribed as a function of latitude on the basis of the previous two experiments, assuming that the sea surface temperatures respond locally and linearly to changes in the surface heat balance. The specified changes in sea surface temperature in the tropics and subtropics were similar to those found by Manabe and Stouffer (1980), but in high latitudes the method proved unreliable and so changes were based on the GFDL experiments. Analysis of the experiments has concentrated on the changes in the hydrological cycle since the temperature change over most of the earth's surface is prescribed.

The warming of the atmosphere is accompanied by an increase in atmospheric moisture, which in the absence of marked changes in circulation leads to increased precipitation (or more accurately, precipitation minus evaporation) in the main regions of low-level atmospheric convergence. Thus, the flux of moisture into high latitudes in winter is enhanced leading to increased precipitation, soil moisture and run off. The equatorward moisture flux associated with the lower branch of the main Hadley cell (the trade winds in the winter hemisphere) is also enhanced, giving enhanced moisture divergence in the winter subtropics where there is a tendency to reduced precipitation. These changes are reflected in the geographical distribution of precipitation; the precipitation increases in the main regions of atmospheric convergence including the mid-latitude depression tracks, especially in winter, and along the intertropical convergence zone and its extension into the continents. Thus precipitation increases over the southern United States, the Sahel and south-east Asia during the northern summer (Fig. 6 (a)) and in eastern South America, South Africa and eastern Australia during the southern summer (Fig. 6 (b)). Precipitation tends to decrease in the regions of enhanced divergence in the subtropics. The pattern of the changes in precipitation is broadly similar to that in the earlier experiment with a uniform increase in sea surface temperatures (Mitchell 1983); this suggests that changes in precipitation are not critically dependent on the detailed structure of changes in sea surface temperature.

Most studies to date have concentrated on the mean changes in climate. The changes in variability may be of greater economic and social importance. Wilson and Mitchell (1987a) analysed changes in variability over western Europe in the third Meteorological Office experiment. They found, for example, that the general reduction in precipitation over southern Europe during the northern summer is the result of both fewer precipitation events and reduced precipitation per event.

3.5 *Detailed studies with simulated cloud*

The earlier GFDL and Meteorological Office experiments used prescribed zonally averaged cloudiness. The parametrization of cloud in climate models is extremely crude, being based on grid-box relative humidity or, in the case of convective cloud, the occurrence of moist convection. Nevertheless, several studies have included model-generated cloud cover (e.g. Hansen *et al.* (1984), Washington and Meehl (1984)). The role of changes in cloudiness in CO_2 experiments has been reviewed by Wetherald and Manabe (1986), and results from a recent Meteorological Office experiment using a low-resolution atmospheric model coupled to a mixed-layer ocean are fairly typical. Cloud amounts increase at upper levels near the model tropopause, due to deeper convection and vertical motion, and decrease in the upper and middle troposphere, particularly in the equatorial mid-latitude convection zones. In effect, the height of the model tropopause is increased. In addition, Wetherald and Manabe (1986) note an increase in low stratus cloud in regions where the atmosphere is inherently stable (e.g. over the winter continents and in the marine boundary layer under the subtropical anticyclones). This they attribute to enhanced evaporation which increases the flux of moisture into the boundary layer where it is trapped under the climatological inversion.

The changes in cloudiness produce a substantial increase in the sensitivity of climate to thermal forcing (Hansen *et al.* 1984). The reduction in total cloud noted in most experiments will warm the surface and troposphere, as noted in section 2.2. Where high cloud is increased at the expense of more highly reflective low cloud, the loss of solar radiation to space is reduced and, because the effective cloud height is also increased, the emission of long-wave radiation to space is also reduced. Hence the warming

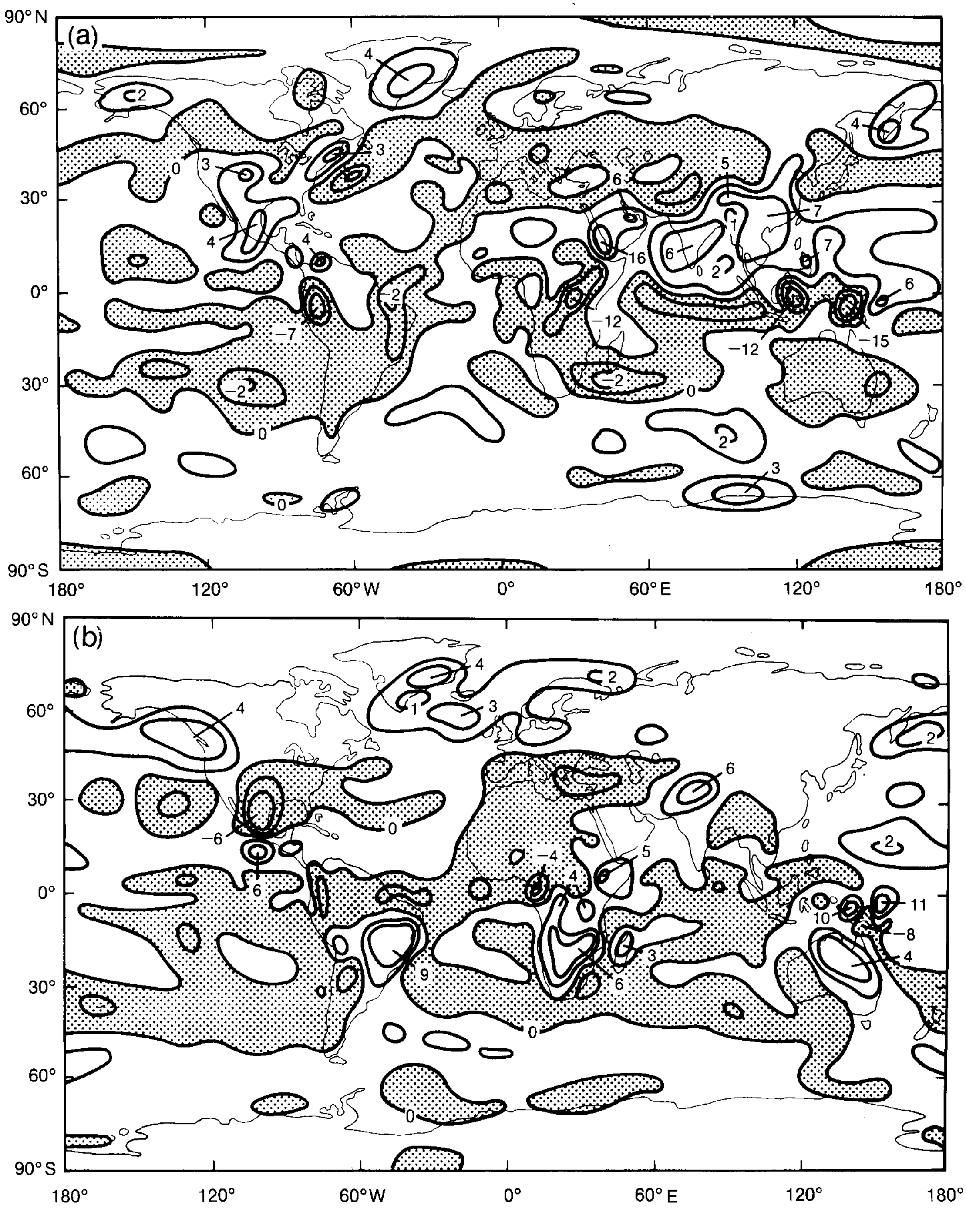

Figure 6. Average changes in precipitation (mm d^{-1}) in the $4 \times CO_2$ experiment with climatological cloud and prescribed changes in the sea surface temperature (Mitchell and Lupton 1984) from (a) June to August and (b) December to February. The areas of decrease are stippled.

of the troposphere and surface is further augmented by enhanced solar heating and reduced long-wave cooling.

The effect of the cloud feedback is such that the global mean temperature changes due to doubling CO_2 is as large as that due to quadrupling CO_2 in a model with fixed cloud (Manabe and Wetherald 1986). The patterns of temperature change in the GFDL $4 \times CO_2$ fixed and $2 \times CO_2$ variable cloud experiments are remarkably similar except in the Antarctic periphery, particularly in the southern summer, where the warming in the $4 \times CO_2$ experiment is smaller, perhaps owing to the underestimation of Antarctic sea-ice extents in the earlier control integration.

A similar though less-marked correspondence exists between the changes in precipitation in the Meteorological Office $4 \times CO_2$ experiment with prescribed cloud (Fig. 6) and a $2 \times CO_2$ experiment with variable cloud (Fig. 7). In both experiments, precipitation increases along the depression tracks

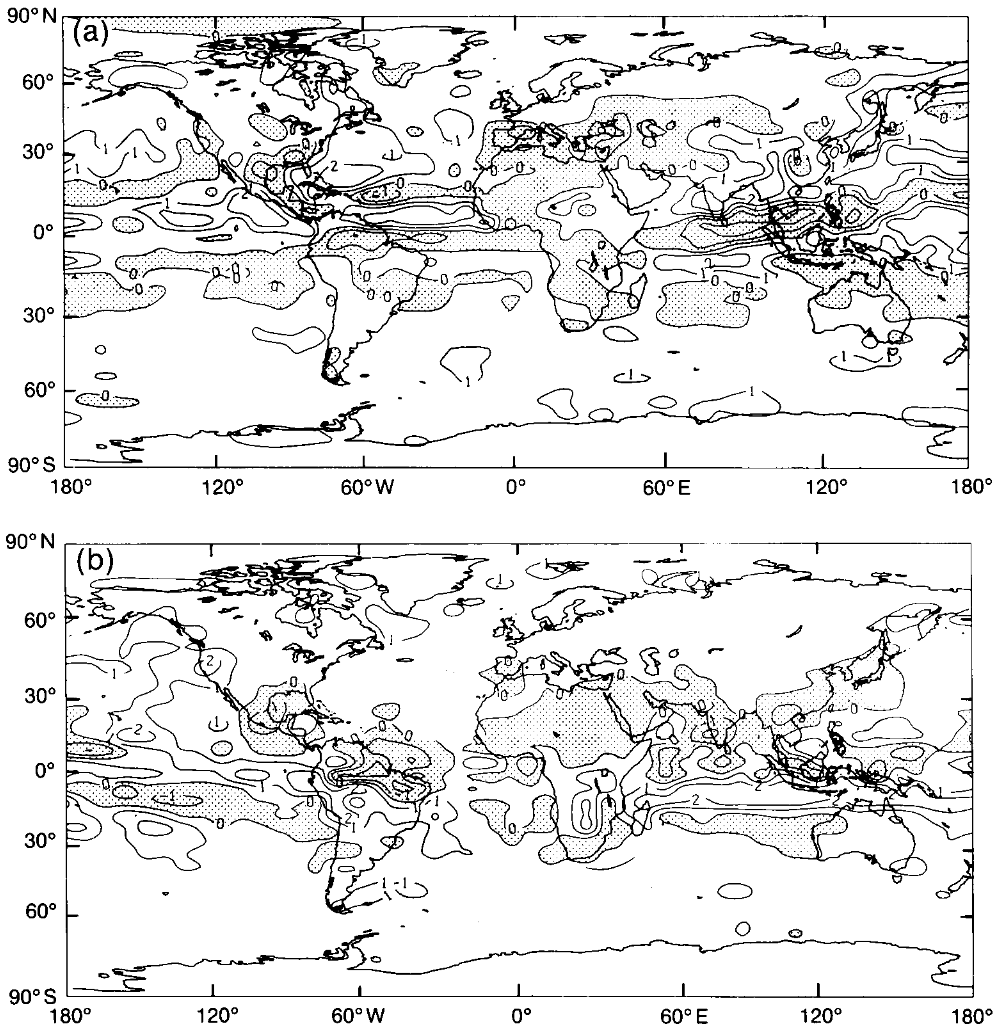

Figure 7. Average changes in precipitation (mm d^{-1}) due to doubling CO_2 (Wilson and Mitchell 1987b) from (a) June to August and (b) December to February. The areas of decrease are stippled.

and in the summer monsoon regions, and changes little or tends to decrease in the subtropics. In general there is a greater tendency for precipitation to increase over the oceans in the $2 \times CO_2$ experiment; since there were considerable differences in the atmospheric models used in the two experiments, this discrepancy is not necessarily due to the differences in the prescription of cloud or sea surface temperature. The problem of model dependence of results is discussed in more detail by Mitchell *et al.* (1987). Note the tendency in the $2 \times CO_2$ experiment for the intertropical convergence zone to shift polewards in the summer hemisphere. (In general, the distribution of changes in precipitation in simulations with increased CO_2 agree less well than the distribution of changes in temperature (Schlesinger and Mitchell 1987). This is largely due to the greater temporal and spatial variability of precipitation and to the large variation in precipitation patterns in control simulations from different models.)

In general, changes in soil moisture are more stable, particularly outside the tropics. As noted earlier, there is a general tendency in the GFDL and Meteorological Office experiments for the land surface in the middle and high latitudes of the northern hemisphere to become drier during summer in the enhanced CO_2 simulations. This is particularly true in studies with model-generated cloud (see Manabe and Wetherald (1986), Wilson and Mitchell (1987b)). One may speculate that the reduction in evaporation associated with the drier surface may reduce boundary-layer cloud, producing a further drying of the surface and so forth.

3.6 *Oceanic effects*

The use of three-dimensional coupled ocean–atmosphere models to study the effects of CO_2 has largely been limited to low-resolution simulations using annually averaged insolation and idealized geography (Spelman and Manabe 1984, Manabe and Bryan 1985). Manabe and Bryan performed six experiments with CO_2 concentrations ranging from 150 to 2400 ppmv. Equilibrium was reached using the acceleration techniques, including those described by Bryan (1984). The zonal mean temperature changes in the upper ocean due to a fourfold increase in CO_2 (Fig. 8) follow those in the atmosphere, with smallest changes in low latitudes due to the effects of moist convection, and the greatest warming in high latitudes due to sea-ice albedo feedback and the weakening of the surface inversion. The large surface warming in high latitudes is propagated into the deep ocean where it is advected equatorwards. Manabe and Bryan comment that the intensity of the model's oceanic meridional circulation changes little for CO_2 concentrations above 300 ppmv. The coefficient of expansion of sea water increases sharply with temperature. Hence, the greater warming in high latitudes is largely compensated by the larger coefficient of thermal expansion in low latitudes and the meridional density gradient is changed little.

3.7 *The transient response*

So far, we have considered only the equilibrium response of climate to enhanced atmospheric CO_2 concentrations. The time-dependent response of climate to an increase in CO_2 concentrations is likely to be slowed by the large thermal inertia of the oceans. Since the effective thermal inertia of the oceans is dependent on the ocean circulation and varies with latitude, it is possible, as suggested by Schneider and Thompson (1981), that the transient response of the climate to enhanced atmospheric CO_2 could differ substantially from the equilibrium response. Spelman and Manabe (1984) investigated the effect of 'switching on' a fourfold increase in CO_2 using synchronous coupling between the ocean and atmosphere (that is, the devices to accelerate convergence to equilibrium were removed) and compared the response with that at equilibrium. After 25 years, the fractional response in the upper atmosphere and surface layer of the ocean was generally uniform with latitude (Fig. 9). The greatest penetration of the warming

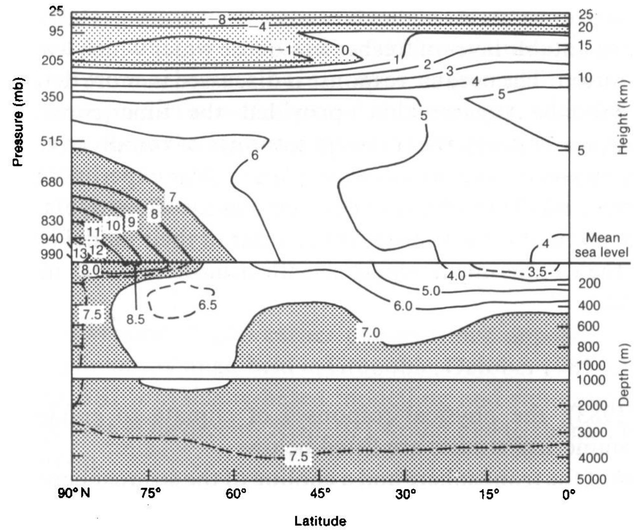

Figure 8. Height–latitude diagram of zonally averaged equilibrium changes in temperature (K) due to quadrupling CO_2 in an idealized coupled ocean–atmosphere model (Spelman and Manabe 1984). Increases of greater than 7 K and decreases are separately delineated.

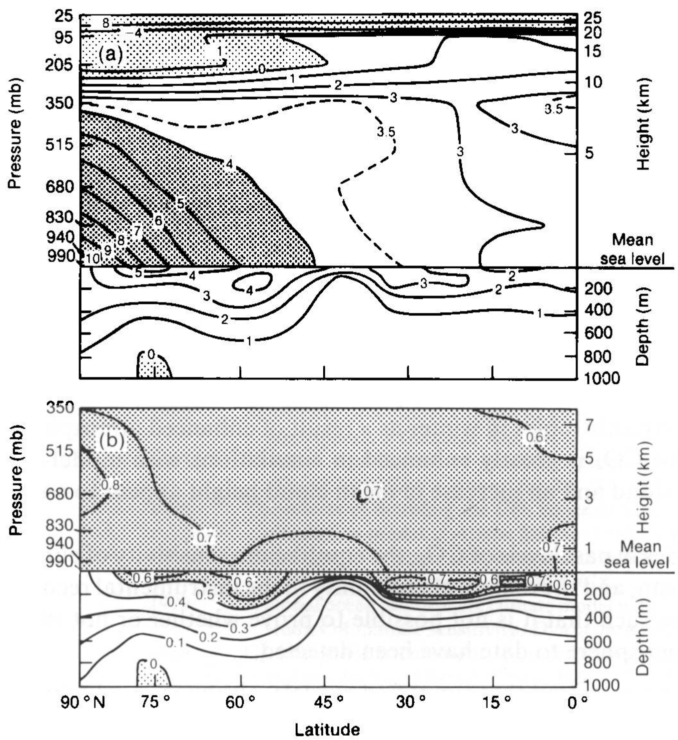

Figure 9. Height–latitude diagram of zonally averaged changes in temperature (a) 25 years after quadrupling CO_2 amounts in an idealized coupled ocean–atmosphere model and (b) fraction of equilibrium response (Spelman and Manabe 1984). Various significant areas are delineated.

in the deep ocean occurred near 55° N. At higher latitudes, the warming is largely confined to the surface layer, due to the presence of a stable layer of fresher less-dense water which was the result of the excess of precipitation over evaporation. The oceanic response is discussed in more detail by Bryan and Spelman (1985). Spelman and Manabe suggest that, provided the time constant for increasing CO_2 concentrations is greater than 25 years, the transient response of zonally averaged temperature should resemble the equilibrium response. The ocean model used in their experiments is highly idealized, does not resolve mesoscale eddies and substantially underestimates the strength of the meridional circulation. As Spelman and Manabe point out, the transient behaviour of their model needs to be verified against observational data and their experiment repeated with a more realistic model before we can have confidence in these results.

4. Concluding remarks

Following Manabe (1983), the physical responses of climate to enhanced CO_2 concentrations determined from recent numerical studies are listed below:

(a) There is a warming of the troposphere and a cooling of the stratosphere because the enhancement of atmospheric CO_2 concentrations increases the opacity of the atmosphere to long-wave radiation, and raises the effective emitting level of the atmosphere.

(b) The annual mean surface warming is largest in high latitudes because of sea-ice and snow–albedo feedbacks, the inherent low-level stability in high latitudes, and perhaps the enhanced advection of latent heat from lower latitudes.

(c) Over the Arctic Ocean and surrounding regions the warming has a large seasonal dependence, and is a minimum in summer. There is little seasonal dependence in temperature changes in low latitudes.

(d) Global mean rates of evaporation and precipitation increase. This is due to enhanced radiative heating at the surface in the warmer, moister, CO_2-enriched atmosphere.

(e) The snow-melt season begins earlier.

(f) Sea-ice is less extensive (and thinner, at least in those studies from which such information is available).

(g) Precipitation and (where reported) run off increase in high latitudes because of the enhanced poleward transport of moisture in the warmer, moister atmosphere.

(h) In most studies to date, soil moisture is reduced over much of the middle- and high-latitude continents of the northern hemisphere in summer. This change is due to one or more of the following factors: earlier snow melt, enhanced evaporation and reduced precipitation. Soil moisture also decreases in northern subtropics in winter as a result of enhanced atmospheric moisture divergence.

(i) The response to CO_2 is greatly enhanced in simulations with model-generated cloud. Both a reduction in total cloud and an increase in mean cloud height appear to contribute to the enhanced surface warming.

(j) The uncertainties in past levels of CO_2, the equilibrium sensitivity of climate to CO_2, the transient response of the ocean, and the temporal variability in the instrumental record of temperature during the last century are such that it is not possible to prove whether or not the climatic effects of CO_2 increases in the atmosphere to date have been detected.

Recent work has demonstrated that simplified models, although invaluable for identifying physical mechanisms, can produce misleading results since they may omit processes relevant to climate change, or they may not weight competing mechanisms correctly. In the same way, it must be recognized that the most sophisticated models in use at present contain many simplifications and approximations which may distort the simulated response to enhanced CO_2. In particular, the horizontal resolution employed in most climate models to date is inadequate to provide an accurate simulation of present-day regional climate, and so such models are unlikely to provide reliable guidance on regional climate change.

Many disciplines are involved in assessing the human consequences of increases in atmospheric CO_2. To do so, they require accurate predictions of potential changes in climate. Numerical models of climate provide the most promising means of making those predictions. Since, unlike those involved in numerical weather prediction, we cannot verify the detailed behaviour of these models using case histories, our confidence in the model's performance must depend on the degree to which it is based on physical principles.

Acknowledgements

This paper is a shortened version of two earlier papers which appeared in the Proceedings of the NATO Workshop 'Abrupt climatic change' held in Grenoble, October 1985 (Dordrecht, Reidel) and the Proceedings of the NATO ASI 'Physically-based modelling and simulation of climate and climatic change' held in Erice, May 1986 (Dordrecht, Reidel). I would like to thank Dr R.W. Riddaway for his help in producing this version.

References

Bryan, K. 1984 Accelerating the convergence to equilibrium of ocean–climate models. *J Phys Oceanogr*, **14**, 666–673.

Bryan, K. and Spelman, M.J. 1985 The ocean's response to a CO_2-induced warming. *J Geophys Res*, **90**, 11679–11688.

Callendar, G.S. 1938 The artificial production of carbon dioxide and its influence on temperature. *Q J R Meteorol Soc*, **64**, 223–240.

Gates, W.L., Han, Y.-J. and Schlesinger, M.E. 1985 The global climate simulated by a coupled atmosphere–ocean general circulation model, preliminary results. *In* Nihoul, J.C.J.(ed); Coupled ocean–atmosphere models. New York, Elsevier.

Hansen, J., Lacis, A., Rind, D., Russell, G., Stone, P., Fung, I., Ruedy, R. and Lerner, J. 1984 Climate sensitivity and analysis of feedback mechanisms. *In* Hansen, J.E. and Takahashi, T. (eds); Climate processes and climate sensitivity. Washington DC, American Geophysical Union.

International Council of Scientific Unions 1979 The global carbon cycle, SCOPE 13. Bolin, B., Degens, E.T., Kempe, S. and Ketner, P. (eds). Chichester, Wiley.

1986 The greenhouse effect, climatic change and ecosystems SCOPE 29. Bolin, B., Döös, B.R., Jäger, J. and Warwick, R.A. (eds). Chichester, Wiley.

Manabe, S. 1983 Carbon dioxide and climatic change. *Adv Geophys*, **25**, 39–82.

Manabe, S. and Bryan, K. 1985 CO_2-induced change in a coupled ocean–atmosphere model and its paleoclimatic implications. *J Geophys Res*, **90**, 11689–11707.

Manabe, S. and Stouffer, R.J. 1980 Sensitivity of a global climate to an increase of CO_2 concentration in the atmosphere. *J Geophys Res*, **85**, 5529–5554.

Manabe, S. and Wetherald, R.T. 1967 Thermal equilibrium of the atmosphere with a given distribution of relative humidity. *J Atmos Sci*, **24**, 241–259.

1975 The effects of doubling the CO_2 concentration on the climate of a general circulation model. *J Atmos Sci*, **32**, 3–15.

1986 Reduction in summer soil wetness induced by an increase in atmospheric carbon dioxide. *Science*, **232**, 626–628.

Manabe, S., Bryan, K. and Spelman, M.J. 1979 A global ocean atmosphere climate model with seasonal variation for future studies of climate sensitivity. *Dyn Atmos and Oceans*, **3**, 393–426.

Marland, G. and Rotty, R.M. 1984 Carbon dioxide emissions from fossil fuels: a procedure for estimation and results for 1950–82. *Tellus*, **36B**, 232–261.

Mitchell, J.F.B. 1983 The seasonal response of a general circulation model to changes in CO_2 and sea temperatures. *Q J R Meteorol Soc*, **109**, 113–152.

Mitchell, J.F.B. and Lupton, G. 1984 A $4 \times CO_2$ integration with prescribed changes in sea temperatures. *Prog Biometeorol*, **3**, 353–374.

Mitchell, J.F.B., Wilson, C.A. and Cunnington, W.M. 1987 On CO_2 climate sensitivity and model dependence results. *Q J R Meteorol Soc*, **113**, 293–322.

Oeschger, H. and Stauffer, B.	1986	Review of the history of atmospheric CO_2 recorded in ice cores. *In* Trabalka, J.R. and Reichle, D.E. (eds); The changing carbon cycle: a global analysis. New York, Springer-Verlag.
Schlesinger, M.E. and Mitchell, J.F.B.	1987	Model projections of equilibrium climatic response to increased CO_2 concentration. *Rev Geophys Space Phys*, **25**, 760–798.
Schneider, S.H. and Thompson, S.L.	1981	Atmospheric CO_2 and climate: importance of the transient response. *J Geophys Res*, **86**, 3135–3147.
Somerville, R.C.J. and Remer, L.A.	1984	Cloud optical thickness feedbacks in the CO_2 climate problem. *J Geophys Res*, **89**, 9668–9672.
Spelman, M.J. and Manabe, S.	1984	Influence of oceanic heat transport upon the sensitivity of a model climate. *J Geophys Res*, **89**, 571–586.
Stephens, G.L.	1978	Radiation profiles in extended water clouds. II: Parameterization schemes. *J Atmos Sci*, **35**, 2123–2132.
US Department of Energy	1985a	Atmospheric carbon dioxide and the global carbon cycle. Report No. DOE/ER-0239. Washington DC, US Dept of Energy.
	1985b	Projecting the climatic effects of increasing carbon dioxide. Report No. DOE/ER-0237. Washington DC, US Dept of Energy.
	1985c	Detecting the climatic effects of increasing carbon dioxide. Report No. DOE/ER-0235. Washington DC, US Dept of Energy.
	1985d	Direct effects of increasing carbon dioxide on vegetation. Report No. DOE/ER-0238. Washington DC, US Dept of Energy.
Washington, W.M. and Meehl, G.A.	1984	Seasonal cycle experiment on the climate sensitivity due to a doubling of CO_2 with an atmospheric general circulation model coupled to a simple mixed-layer ocean model. *J Geophys Res*, **89**, 9475–9503.
Washington, W.M., Semtner, A.J. jun., Meehl, G.A., Knight, D.J. and Mayer, T.A.	1980	A general circulation experiment with a coupled atmosphere, ocean and sea ice model. *J Phys Oceanogr*, **10**, 1887–1908.
Wetherald, R.T. and *Manabe, S.*	1986	An investigation of cloud cover change in response to thermal forcing. *Clim Change*, **8**, 5–23.
Wilson, C.A. and Mitchell, J.F.B.	1987a	Simulated climate and CO_2-induced climate change over western Europe. *Clim Change*, **10**, 11–42.
	(1987b)	A $2 \times CO_2$ climate sensitivity experiment with a global climate model including a simple ocean. (To appear in *J Geophys Res.*)

551.524.37(412):551.507.362.2

Satellite images of the distribution of extremely low temperatures in the Scottish Highlands

J. McClatchey, A.M.E. Runacres* and P. Collier

Department of Geography, Portsmouth Polytechnic

Summary

Temperatures below −20 °C have been recorded at stations in the Scottish Highlands on a number of occasions in the last six years. This paper describes the use of data from the Advanced Very High Resolution Radiometer on board the NOAA series of satellites to investigate the distribution of such low temperatures in the Highlands, and shows that even lower temperatures may have occurred than were recorded at any climatological stations.

1. Introduction

In three out of the last five winters since the UK extreme minimum screen temperature of −27.2 °C was last equalled on 10 January 1982 at Braemar, minima below −20 °C have been recorded at one or more stations in the Scottish Highlands. This paper examines the use of data from the Advanced Very

* Now at University College, Swansea

High Resolution Radiometer (AVHRR) on board the NOAA series of satellites to investigate the distribution of such low temperatures, and to determine whether even lower values are likely to have occurred at places where no climatological station is sited.

2. Problems in data analysis

2.1 *Satellite thermal imagery*

The AVHRR data consist of radiance values for each of five channels with a nadir instantaneous field of view of 1.1 km × 1.1 km and, although this spatial resolution is not as high as that available from Landsat for example, the temporal resolution is much greater with two satellite overpasses per 24 hours as compared to Landsat's one in 16 days. The thermal infra-red imagery is split into three channels (Channels 3, 4 and 5) of which Channels 4 and 5 are of most use in estimating surface temperatures. The spectral characteristics of the NOAA AVHRR are given by Lauritson *et al.* (1979).

An archive of AVHRR data is held by the Department of Electrical Engineering and Electronics at the University of Dundee from whom a computer tape of the digital information for a particular date can be obtained.

The radiance values from each channel come in the form of a 10-bit count giving a range of values from 0 to 1023. Using the method of Lauritson *et al.* (1979), these can be converted to equivalent black-body temperatures termed brightness temperatures. These brightness temperatures differ from actual surface temperatures by a variable amount which depends on, in particular, the effects of atmospheric attenuation and the values of surface emissivity. Also, as clouds effectively act as black bodies for terrestrial wavelengths, only cloud-free pixels (the approximately 1.1 km × 1.1 km picture elements) can be used in determining surface temperatures. Despite these problems, AVHRR data have been successfully used to estimate sea surface temperatures (Singh and Warren 1983). Also Pescod *et al.* (1986) reported that the operational use of AVHRR data in the production of maps of sea surface temperature is being investigated at the Meteorological Office.

2.2 *Surface emissivity*

The use of AVHRR imagery for determining the temperature of water surfaces is simplified by the fact that a constant emissivity can be assumed. Unfortunately, the same is not true for land surfaces and, although Kalma *et al.* (1986) felt justified in assuming a constant emissivity across their study area in New South Wales, Cooper and Petersen (1985) working in New Mexico estimated that an error of 2 °C or more was introduced as a result of emissivity changes across their images. This problem does not exist in areas with a permanent snow cover as the emissivity can again be assumed to be constant. Thermal imagery has therefore been successfully used in areas such as the Antarctic (Thomas and D'Aguanno 1985).

Although snow cover in the Scottish Highlands is certainly not permanent, the dates with minima below −20 °C investigated in this study all occurred during periods of widespread snow cover with depths of at least 20 cm and often more than 30 cm recorded at all the climatological stations in the study area (except on 27 February 1986 when one station at the fringe of the area recorded only 14 cm of lying snow). The assumption was therefore made that emissivity would be constant across the study area.

The value of snow-surface emissivity suggested by various authors ranges from 0.97 to 1.00 with a value of 0.99 being the most frequently quoted (e.g. Aguado 1985 or Müller 1985). Roach and Brownscombe (1984) suggested, however, that an emissivity of unity was a good approximation for snow surfaces and, as one of the dates in this study (10 January 1982) is the same as that investigated by them, an emissivity of 1.00 was also used in this study to enable a direct comparison to be made with their results.

An emissivity of less than 1.00 will reduce the brightness temperature calculated from the AVHRR radiance value and therefore will suggest a surface temperature somewhat lower than the true value. If the snow-surface emissivity was taken as 0.99 this would decrease the apparent surface temperatures recorded by the radiometer by about 0.6 °C (at temperatures of the order of −20 °C). The results quoted later are therefore unlikely to be greatly affected by the use of an emissivity of 1.00 rather than 0.99.

2.3 *Atmospheric attenuation*

Cloud cover obviously presents the greatest problem in using AVHRR data to determine surface temperatures, but even when clouds are not present attenuation of the transmitted radiation occurs principally due to infra-red absorption bands of water vapour. It is possible to calculate the amount of attenuation for a given scene, but this requires a knowledge of the structure of the atmosphere at the place and time of observation. A number of techniques are available to overcome this problem, the most commonly used being multi-spectral scanning and the calibration of the satellite data with *in situ* observations.

Multi-spectral scanning makes use of two or more channels to estimate attenuation as each channel will be affected to a different degree by the same attenuating conditions. Various algorithms have been published, for example those by Robinson (1985), and a number of these were used in this study.

Calibration with *in situ* observations makes use of measurements of temperatures at a series of points on the image to determine differences between the brightness temperatures and observed temperature at the surface. These differences indicate the amount of attenuation by the atmosphere, and the average attenuation can then be used to estimate surface temperatures in parts of the scene where no surface observations were taken. Such *in situ* data are usually used in conjunction with multi-spectral scanning and are generally considered essential to validate algorithms (Callison and Cracknell 1982).

2.4 *Earth location*

The location of any pixel in the scene can be computed from the satellite navigation data. The predicted position of the satellite above the earth can, however, have an along-track error of over 10 km (Pescod *et al.* 1986) which results in some location error. Roach and Brownscombe (1984), for example, reported that the NOAA-7 image taken at 0417 GMT on 10 January 1982 appeared to have about a 2 km mismatch between the navigation data location and topography in the Spey Valley (on the assumption that the coldest air was in the valleys). Pescod *et al.* (1986) corrected for such errors by computing a coastline and comparing that with the actual coastline on the image, the location information then being recomputed to include the offsets between the two coastlines (coastlines are used as the contrast between land and water surfaces makes them easy to identify). Such a procedure is obviously only possible when there is at least some cloud-free coast within the image, but in the present study this was not a problem as virtually the whole of northern and eastern Scotland was cloud free in each of the four cases. In fact, it was also possible to use a number of the Scottish lochs (notably Loch Ness, Loch Laggan and Loch Ericht) which provided clear linear features on the images and, together with the coastlines, these greatly aided accurate registration. Given their clarity, these features were used in preference to the satellite navigation data for determining pixel locations. It should be noted, however, that if the image is towards the edges of the large swath of information produced by the satellite then considerable distortions occur as a result of the earth's curvature (the pixel size is increased too); therefore pixels can only be effectively located in this way if they are from images in the centre of the swath.

3. Results

3.1 *Dates of investigation*

Four dates on which low minima were recorded in the Scottish Highlands were included in the investigation. There were a few other dates on which similarly low minima were recorded but these were rejected either because of cloud contamination found by inspection of the image, or because the area under study was distorted due to its being towards the edge of the image swath. It can, however, be difficult to discriminate between low cloud or fog and a cloud-free snow surface at night, and therefore the weather and cloud-amount reports recorded at stations in the area were also examined to confirm that cloud and fog were not present. The dates finally chosen have the advantage of being completely independent as they are all from different years. The dates and the screen minimum temperatures observed at climatological stations within the area are given in Table I.

Table I. *Dates of satellite images and screen minima (°C) for those dates recorded at stations within the study area*

	10 Jan. 1982	20 Jan. 1984	25 Jan. 1985	27 Feb. 1986
Station		Screen minimum temperatures		
Aviemore*		−20.6	−18.9	−19.5
Braemar	−27.2	−21.3	−20.1	−18.2
Dalwhinnie	−18.0	−19.1	−16.4	−14.4
Grantown-on-Spey	−25.7	−23.6	−20.1	−21.2
Lagganlia	−24.1	−23.5	−22.0	−20.6

*Aviemore synoptic station was not opened until after January 1982.

3.2 *AVHRR estimated temperatures*

The images for the four dates were processed to produce brightness temperatures; this processing included the non-linearity correction suggested by Lauritson *et al.* (1979). The brightness temperatures for each of the pixels in which the climatological stations were sited were then compared with the screen minima recorded at these stations. The screen minima were used even though the grass minima would be more likely to be closer to the radiative skin temperatures measured by the satellite. This decision was made because an examination of the climatological records suggested that there may have been some inconsistency in the exposure of the grass minimum thermometers at the various stations.

The brightness temperatures differ from the screen minima for a number of reasons:

(a) Atmospheric attenuation affects the recorded radiance values.
(b) The satellite overpass time does not necessarily correspond with the time of screen minimum.
(c) The satellite sensor averages the radiance value over a 1.1 km × 1.1 km pixel whereas the screen minimum is a point value.
(d) Surface temperatures may not be the same as screen minima recorded at 1.2 m.
(e) There may be an error in the location of the station on the image.
(f) Noise and other errors in the measurement systems.

The calculated brightness temperatures for AVHRR Channels 3, 4 and 5 were all higher than the recorded screen minima, which is rather unusual as in most studies the brightness temperatures are lower than *in situ* observations. This discrepancy probably arises for two reasons. Firstly, the time of the satellite overpass was either before or after the time the screen minima were reached (as the 0900 GMT dry-bulb temperatures were all higher than the minima, the screen minima probably occurred before

0900 GMT) and secondly, atmospheric attenuation was small as all occasions had low values of precipitable water (as recorded by the midnight radiosonde ascent at Shanwell). Since attenuation was small, the main difference was almost certainly as a result of the time of overpass not coinciding with the time of screen minimum, a conclusion which tends to be confirmed by the lowest mean offset value for Channel 4 (the mean difference between recorded screen minima and brightness temperatures) being found on 25 January 1985 when the satellite overpass was at 0841 GMT. This overpass was less than 30 minutes after sunrise and probably not much more than this after screen minima were recorded. It should also be noted that Channel 4 is the least likely to be affected by attenuation by any variation in the amount of water vapour as its waveband range lies within the range of the minimum values of the effective mass-absorption coefficients for water vapour (Ramsey *et al.* 1982).

The differences between the screen minima and the computed Channel 4 brightness temperatures, the offsets, are given in Table II along with the root-mean-square (r.m.s.) value of the variations from this mean (following Bowers *et al.* (1982)).

Table II. *Offsets between AVHRR Channel 4 brightness temperatures and recorded screen minima (°C) for the same dates as Table I*

	10 Jan. 1982	20 Jan. 1984	25 Jan. 1985	27 Feb. 1986
Satellite	NOAA-6	NOAA-7	NOAA-6	NOAA-9
Time (GMT) of overpass	0925	0450	0841	0410
Station				
Aviemore*		1.0	0.7	1.0
Braemar	2.5	1.5	0.0	1.9
Dalwhinnie	2.2	1.5	0.4	1.4
Grantown-on-Spey	2.2	1.1	0.0	0.8
Lagganlia	3.4	2.4	0.6	3.9
Mean offset	2.6	1.5	0.3	1.8
r.m.s. error	0.49	0.49	0.30	1.12
Mean offset (excluding Lagganlia)	2.3	1.3	0.3	1.3
r.m.s. error	0.14	0.23	0.30	0.42

*Aviemore synoptic station was not opened until after January 1982.

The mean offsets are given with and without the values from Lagganlia as the Lagganlia offsets were noticeably higher than the other stations, particularly on 27 February 1986. This difference is almost certainly the result of local site conditions and visits to the stations suggest that there is greater local shelter at Lagganlia than at the other sites.

The mean offsets were then subtracted from the Channel 4 brightness temperatures for each pixel to create a map of the distribution of minimum temperatures for each of the four dates. Although it made little difference on three of the dates, the offsets used were those excluding Lagganlia, as not using that offset gave a substantial improvement in the r.m.s. error on 27 February 1986.

Various published multi-spectral attenuation algorithms for calculating surface temperatures were also used to see if it was possible to obtain better results as measured by the r.m.s. error from the observed screen minima; see for example Robinson (1985) or Bowers *et al.* (1982). No multi-spectral imagery was available on 25 January 1985 due to an error on Channel 3 and the algorithms which included Channel 5 brightness temperatures could not be used on 10 January 1982 as NOAA-6 does not have a separate Channel 5. However, of the 11 different algorithms tested, even the best of them had r.m.s. errors more than twice as large as those obtained by simple subtraction of a mean offset from the Channel 4 brightness temperatures (even those with the Lagganlia values included). This was not an unexpected result as the multi-spectral algorithms are normally derived for typical mid-latitude or global maritime atmospheric conditions but it did confirm that such algorithms are of little use during conditions of extreme cold.

3.3 *Density slicing*

The calculated pixel values were then density sliced using the image-processing system for a Sirius microcomputer with Pluto colour board written at the Department of Geography, Portsmouth Polytechnic. This density slicing allows a range of pixel-count values to be assigned a single intensity value. A careful choice of intensity values enables a detailed thermal map to be produced with an uncertainty as measured by the r.m.s. errors of less than 0.5 °C. It was therefore felt valid to density slice at 0.5 °C intervals but this would have caused overcomplication over the whole image as it is difficult to assign more than 30 separate colours which can be clearly distinguished. However, as the study was concerned with the distribution of very cold temperatures, an uneven density slice was carried out with the 0.5 °C intervals used only for temperatures below −20 °C.

Although the map of temperature distribution was very detailed, an isotherm interval of 5.0 °C was chosen for the printed maps. This interval provided a good summary of the overall pattern, demonstrating the match with topography, and it was also the interval used by Roach and Brownscombe (1984) in their investigation of minimum temperatures on 10 January 1982.

3.4 *Errors*

Despite the detail available by density slicing, it is important to make some estimate of the reliability of the derived temperature distribution. Errors can arise from each stage of the processing so that there are *in situ* observational uncertainties depending on the instruments used and their exposure, uncertainties introduced in locating the ground stations on the image and errors arising from the radiometric measurements.

As far as the *in situ* observations are concerned, the instruments and their exposure were all standardized so any error is likely to be small, and less than 0.1 °C. Location errors, however, are not so easy to quantify but, following the example of Cooper and Petersen (1985), average differences were calculated between the pixels containing the climatological stations, and their eight adjacent neighbours. This error was 0.5 °C. Errors which arise from the radiometric measurements include:

(a) Instrument calibration and precision (quoted as 0.31 °C by Lauritson *et al.* (1979)).
(b) Errors in the offset values (r.m.s. errors were found to be less than 0.5 °C).
(c) Emissivity errors (spatial variations were assumed to be negligible in this study).
(d) Atmosphere attenuation (spatial variations assumed negligible).

A measure of the total uncertainty can be obtained by the root sum square method used by Cooper and Petersen (1985) which takes the square root of the sum of squares of the error terms. In this study the root sum square value was 0.78 °C and therefore isotherms as drawn should be correct to within 1.0 °C.

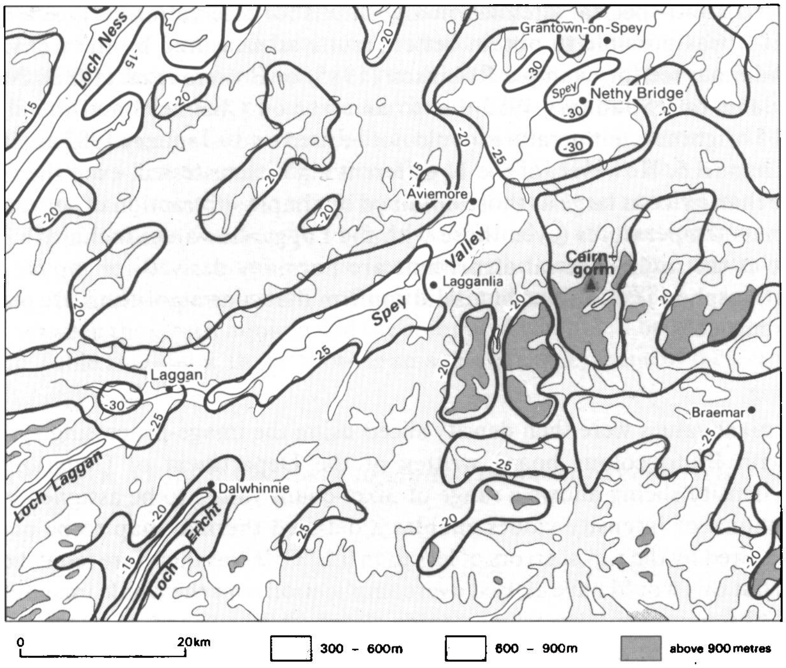

Figure 1. Isotherms (°C) showing the distribution of temperature in the Scottish Highlands on 10 January 1982 derived from NOAA-6 AVHRR data (0925 GMT overpass).

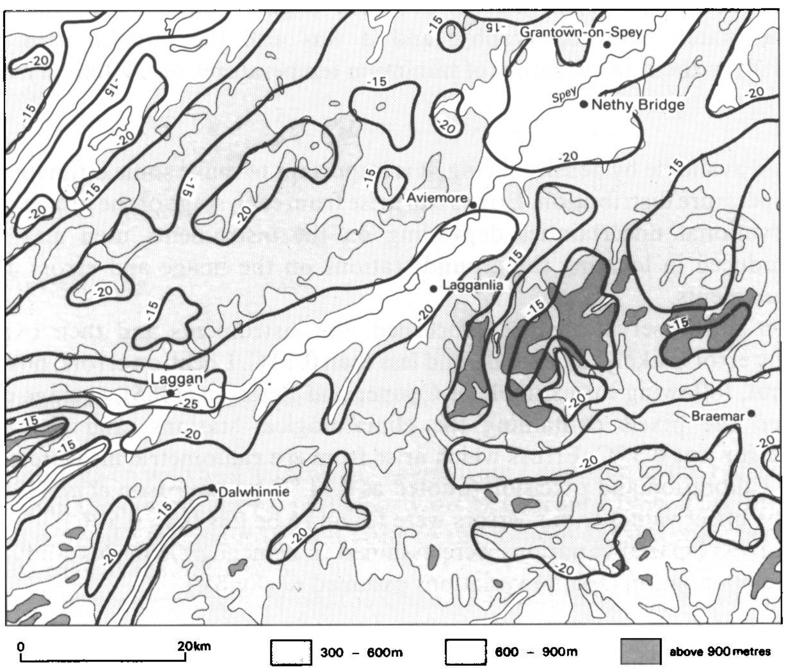

Figure 2. Isotherms (°C) showing the distribution of temperature in the Scottish Highlands on 20 January 1984 derived from NOAA-7 AVHRR data (0450 GMT overpass).

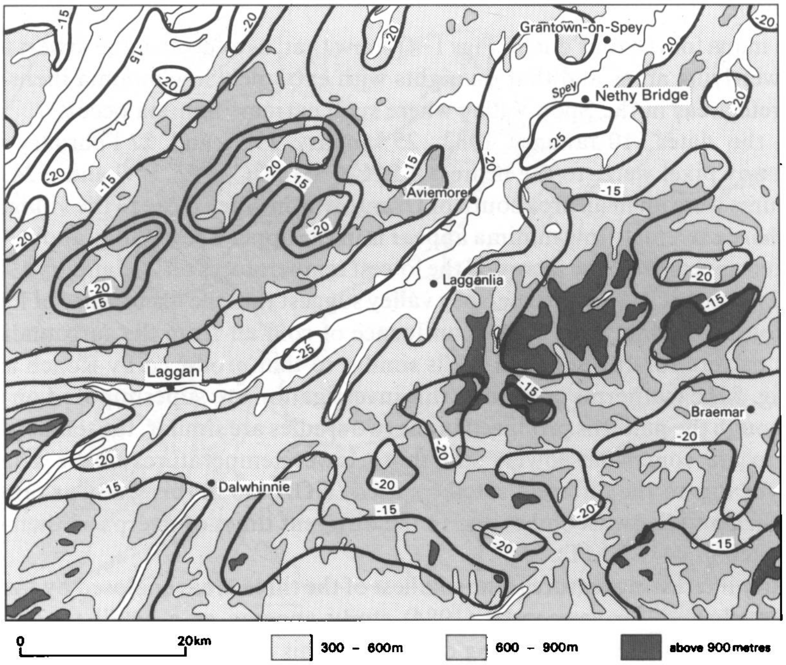

Figure 3. Isotherms (°C) showing the distribution of temperature in the Scottish Highlands on 25 January 1985 derived from NOAA-6 AVHRR data (0841 GMT overpass).

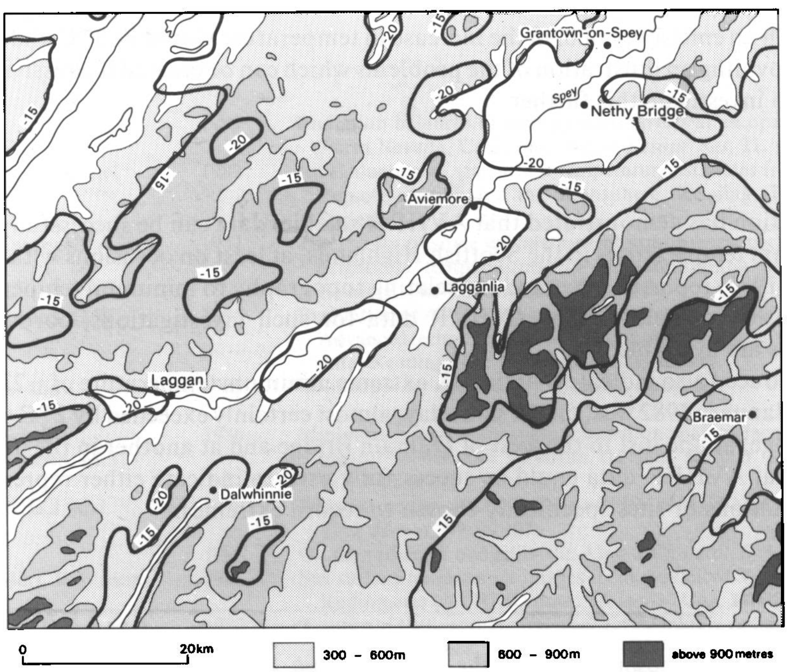

Figure 4. Isotherms (°C) showing the distribution of temperature in the Scottish Highlands on 27 February 1986 derived from NOAA-9 AVHRR data (0410 GMT overpass).

3.5 *Isotherm maps*

The isotherm maps for the four dates (Figs 1–4) show that, as expected, the lowest temperatures were found in the lower-lying areas and that on nights with extremely low minima there do appear to be a number of discrete areas in the Spey Valley where such extreme minima occur.

On three of the dates, 10 January 1982, 25 January 1985 and 27 February 1986, the lowest temperatures in any pixel were (to the nearest 0.5 °C) −31.5 °C, −25.5 °C and −24.0 °C respectively. These temperatures were all in an area south of Grantown-on-Spey close to the village of Nethy Bridge. Another area where extremely low minima appear is in the upper Spey Valley about 4 km to the west of Laggan. That area appears to have recorded the lowest temperatures on 20 January 1984 (−26.0 °C) and 10 January 1982 (−30.5 °C). Visits to the Spey valley suggest that the occurrence of low temperatures at these two locations is probably due to the confluence of cold air from the surrounding areas.

The isotherm pattern for 10 January 1982 is similar to that produced by Roach and Brownscombe (1984) and in Fig. 5 the isotherms created in this investigation are superimposed on top of those from their study. Although the patterns produced in the two studies are similar, the temperatures estimated in this investigation are somewhat lower, and those lower temperatures cover a larger area. These differences may be due to the different satellites used (NOAA-6 in this study as opposed to NOAA-7 data used by Roach and Brownscombe) and to the different times of overpass (their calculations were based on data taken at 0417 GMT).

One particularly interesting feature is the smallest of the three areas enclosed by the −30 °C isotherm which in the Roach and Brownscombe (1984) study appears as a small tongue of cold air (the intersection is shown by the cross-hatching on Fig. 5). This area appears to be centred on Abernethy Forest which might not be expected to record the lowest temperatures.

However, Henderson-Sellers and Robinson (1986) quote an infra-red emissivity of 0.88 for snow-covered vegetation which would give a temperature 7 °C warmer than that estimated using an emissivity of 1.0. Even with an emissivity of 0.95 the increase in temperature would be 3 °C and it may be that this small area is providing an illustration of the problems which can be created if emissivity is not constant. It is intended to investigate this further.

4. Conclusions

The investigation has demonstrated that AVHRR satellite data can be successfully used to produce maps of minimum temperatures in the Scottish Highlands, at least on occasions with widespread snow cover. Tabony (1985) reported a method for relating topography to minimum temperatures but it may prove rather easier to make use of AVHRR data for such investigations, particularly if suitable emissivity values are available.

The maps produced also indicate that the UK extreme minimum temperature of −27.2 °C recorded at Braemar on 10 January 1982 was, on the same day, almost certainly exceeded by 2 °C or more at one site near Nethy Bridge, at one just to the west of Dulnain Bridge and at another in the upper Spey Valley. This suggests that AVHRR data could be successfully used to indicate either representative sites for climatological stations or sites specifically chosen to record extremes.

Acknowledgements

The authors would like to thank R. Reynolds of the Department of Meteorology, University of Reading for his helpful comments and the Cartographic Unit of the Department of Geography, Portsmouth Polytechnic for drawing the maps.

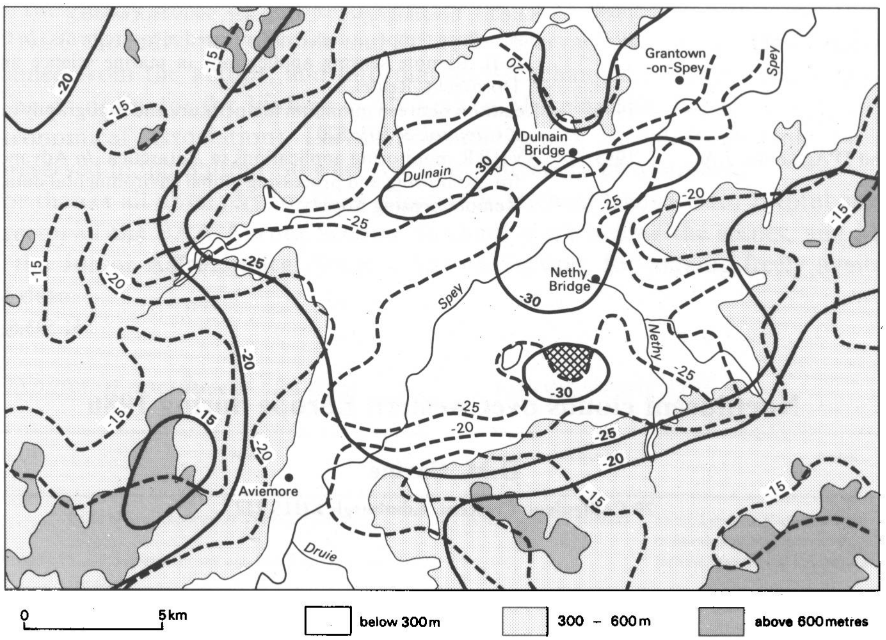

Figure 5. Isotherms (°C) for part of the Spey Valley on 10 January 1982. Dashed isotherms are those given by Roach and Brownscombe (1984) and solid isotherms are those produced in this study. The cross-hatching is an area of interest discussed in the text.

References

Aguado, E. 1985 Radiation balances of melting snow covers at an open site in the Central Sierra Nevada, California. *Water Resour Res*, **21**, 1649–1654.

Bowers, D.G., Crook, P.J.E. and Simpson, J.H. 1982 An evaluation of sea surface temperature estimates from the AVHRR. *In* Remote sensing and the atmosphere. Reading, The Remote Sensing Society.

Callison, R.D. and Cracknell, A.P. 1982 The results of some calculations of atmospheric corrections to AVHRR brightness temperatures. *In* Remote sensing and the atmosphere. Reading, The Remote Sensing Society.

Cooper, D.I. and Petersen, G.W. 1985 Evaluation of AVHRR sensor for monitoring land surface temperatures. *In* Advanced technology for monitoring and processing global environmental data. Reading, The Remote Sensing Society.

Henderson-Sellers, A. and Robinson, P.J. 1986 Contemporary climatology. Harlow, Longman.

Kalma, J.D., Laughlin, G.P., Green, A.A. and O'Brien, M.T. 1986 Minimum temperature surveys based on near-surface air temperature measurements and airborne thermal scanner data. *J Climatol,* **6**, 413–430.

Lauritson, L., Nelson, G.J. and Porto, F.W. 1979 Data extraction and calibration of TIROS-N/NOAA radiometers. NOAA, *Tech Memo*, NESS 107.

Müller, H. 1985 On the radiation budget in the Alps. *J Climatol*, **5**, 445–462.

Pescod, R.W., Saunders, R.W. and Eyre, J.R. 1986 Sea surface temperature images from Advanced Very High Resolution Radiometer (AVHRR) data. *Meteorol Mag*, **115**, 318–325.

Ramsay, J.W., Chiang, H.D. and Goldstein, R.J. 1982 A study of the incoming longwave atmospheric radiation from a clear sky. *J Appl Meteorol*, **21**, 566–578.

Roach, W.T. and Brownscombe, J.L. 1984 Possible causes of the extreme cold during winter 1981–82. *Weather*, **39**, 362–372.

Robinson, I.S.	1985	Satellite oceanography. Chichester, Ellis Horwood.
Singh, S.M. and Warren, D.E.	1983	Sea surface temperatures from infrared measurements. *In* Cracknell, A.P. (ed); Remote sensing applications in marine science and technology. Dordrecht, Reidel.
Tabony, R.C.	1985	Relations between minimum temperature and topography in Great Britain. *J Climatol*, 5, 503–520.
Thomas, I.L. and D'Aguanno, J.A.	1985	AVHRR monitoring applications in Antarctica. *In* Advanced technology for monitoring and processing global environmental data. Reading, The Remote Sensing Society.

551.593.653(4):551.506.1

Noctilucent clouds over western Europe during 1986

D.M. Gavine

29 Coillesdene Crescent, Edinburgh EH15 2JJ

Summary

The sightings of noctilucent clouds reported to the Aurora Section of the British Astronomical Association during 1986 are presented.

Table I summarizes the noctilucent cloud (NLC) reported to the Aurora Section of the British Astronomical Association (BAA) during 1986. The times (UT) are of reported sightings, not necessarily the duration of a display. Hourly sky reports are no longer received from meteorological stations; consequently negative nights are now based on the judgement of two or more experienced observers with clear or nearly clear sky, watching throughout the whole period during which NLC is likely to occur, and in the case of Britain, north of 54° N. Table II lists those nights adjudged to be negative.

The large number of sightings, despite a summer beset with tropospheric cloud in Britain, suggests a high incidence of the phenomenon in 1986. The network of observers has been extended, both geographically and in numbers. British data came from 26 amateur astronomers and other individuals, and 12 meteorological stations. The Finnish network now comprises 20 single observers and 6 teams, covering latitudes 60–65° N, longitudes 21–30° E. They employ data storage systems and produce a detailed annual report. The Danish group of 5 is co-ordinated by Mr J. Østergaard Olesen at Rønne in Bornholm. Mr Olesen and Mr Holger Andersen continue to submit reports which are models of clarity, and their outstanding colour photographs, especially of panoramic views of NLC, have been exhibited at the BAA and other meetings.

We are very pleased to welcome to the survey the Royal Netherlands Meteorological Institute, who contributed NLC sightings from 21 stations. Photographs of the 1986 displays have already been published (Zwart 1986). In addition, NLC reports have been received from two Canadian observers, Mr Brown and Mr Zalcik; these are briefly mentioned for comparison. Following a popular article (McConnell 1987) several amateur observers in Canada have expressed a desire to participate, and the development of a North American network seems likely.

Thirty-four definite NLC were observed in Finland, 29 in Britain, 17 in Denmark and 5 in the Netherlands. Parallactic photography was achieved on the spectacular display of 23/24 July using fixed cameras at Milngavie (Dr Simmons), Edinburgh (Dr Gavine) and Aberdeen (Dr Gadsden). Dr Gadsden also carried out time-lapse photography and TV polarimetry.

Because of the greatly increased volume of data for 1986 it has been found necessary to omit from the summary of NLC the individual altitude and azimuth observations. Full data on individual displays may be obtained from the author, and information is exchanged between the Finnish and British networks. The co-ordinator for Finland is Mr Veikko Mäkelä, Tähtitieteellinen yhdistys URSA ry (URSA Astronomical Association), Laivanvarustajankatu 3, SF-00140 Helsinki 14. All data are ultimately preserved in the Balfour Stewart Archive, University of Aberdeen.

The author thanks all observers for their efforts, Dr Michael Gadsden for helpful advice, Mr Ron Livesey, Director of the BAA Aurora Section, for hard work behind the scenes, and Mr Neil Bone, Director of the Junior Astronomical Society Aurora Section, for making freely available his own collection of data.

Table I. *Displays of noctilucent clouds over western Europe during 1986*

Date — night of	Times UT	Notes
28/29 Apr.	2010	Faint billow suspected at Tapiola, Finland.
28/29 May	2130–0000	Small, rather faint veil and bands at Turku and Helsinki.
6/7 June	2310–0200	Faint bands and billows, mostly in tropospheric cloud, Scotland and N England.
10/11	2330	Faint NLC up to zenith at Wick.
13/14	2030–0225	Moderately bright display, all forms, seen throughout Britain down to Worcester, Denmark and Netherlands. Strong billow structure photographed by Mr Andersen at Vildbjerg.
14/15	0000–0100	Faint band at Wick; no NLC at Aberdeen 2200–2305.
15/16	2240	Very faint NLC visible through binoculars at Rønne.
16/17	2100–2145	Very faint NLC visible through binoculars at Rønne.
18/19	2100–0200	Bright display well into the southern sky in S Finland, observed in Estonia. Faint bands visible in Britain to 53.5° N and Deventer, Netherlands.
19/20	2140–2323	Faint NLC at Helsinki, maximum altitude 75° at 2302. Faint bands at Castleford (Yorks) and Rønne.
21/22	2110	Bands in broken cloud at Rønne.
22/23	2125–2320	Faint bands at Helsinki. NLC suspected in cloud gaps at Sale (Manchester) but negative at Stirling.
23/24	2119–0200	Faint bands in zenith and SW sky at Helsinki. Magnificent display, all forms, bright, over Denmark. Faint NLC at Rotterdam. Billows up to 10° at Edmonton, Canada.
24/25	2150–0045	Faint bands in tropospheric cloud gaps, Edinburgh; faint NLC in Denmark. Small faint band and billow display at Vantaa (Finland) after 0130 local time. Bands and billows to 7° at Edmonton.
25/26	2155–2345	Small, diminishing and fading bands and billows in Britain, visible down to 52° N.
26/27 June	2145–0015	Faint; bands at Morpeth, Northumberland, billows at Bornholm. Veil, bands and billows east of Helsinki, increasing towards dawn.
27/28	0012–0050	Faint NLC patch suspected in zenith at Wick, very faint bands and billows at Vildbjerg. Faint billows at Edmonton.
28/29	2100–0250	Large bright display, all forms, in England and Denmark, observed in tropospheric cloud in Scotland. Reported at 11 Netherlands stations. In Helsinki one NLC area in zenith and S sky, another low in N with strong billows in W. Bright at Morpeth with billows and whirls but became fainter from 2350.
29/30	2215–0200	Bright bands seen at Todmorden (Yorks), widespread display overhead in haze at Aberdeen. Faint blue–green patch at Rønne, faint bands at Helsinki after 0100 local time.
1/2 July	2120–0255	Moderately bright, extensive display, bands and some billows, observed from 10 British and 2 Danish stations, also Fishery Protection Vessel *Jura* at 59° N, 5.5° W. Faint forms seen S of zenith near dawn at Bedford. Small faint patches at Tapiola and Vantaa, Finland.
2/3	2309–0215	Faint bands and a few billows in cloud gaps in N England.
3/4		Bands and billows up to 15° at Edmonton, Canada.
5/6	2230–0232	Faint NLC, mainly bands, N Britain. Suspect bands at Tapiola.
6/7	2320–0240	Faint bands at Bornholm and in N Britain. Bright NLC in cloud gaps at Turku.
7/8	2115–2300	Bands at Todmorden. Bright widespread display at Helsinki and Turku, all forms in E sky from horizon to zenith.
8/9	2115–0240	Faint bands reported at Todmorden but no NLC visible at Aberdeen at 2230. Small faint NLC in S Finland.

Date — night of	Times UT	Notes
10/11 July	2130–0100	No NLC at Stirling 2300 but NLC in cloud gaps, Linton-on-Ouse (Yorks) 0100. NLC in cloud gaps, Denmark. Faint widespread NLC at Kustavi, SW Finland.
11/12	2100–0154	Bright display, all forms, Denmark and Twenthe (Netherlands).
12/13	2135–0130	Small bands in Orkney. Bright display, all forms, in S Finland and Kuopio area. NLC at Fort McMurray, Canada.
13/14	2155–0030	Bright bands and billows at Bornholm. Faint bands at Fort McMurray.
15/16	2110–2315	Widespread and bright display in Finland, all forms. Up to zenith at Helsinki, all-sky at Rautalampi and Kuopio.
16/17	2210–0204	Faint to moderate NLC over Britain down to Yorkshire, mainly bands, some billows and whirl structure. Small faint veil in S Finland after 0030 local time.
17/18	2100–0230	Negative at Aberdeen 2315 but faint veil suspected overhead at Todmorden 2135–2159, and definite NLC in cloud gaps 0215–0230. Small bright NLC in E Finland.
18/19	0240–0315	Faint NLC patch suspected overhead at Todmorden.
19/20	2125–0240	Moderate display, all forms, in cloud gaps at Morpeth, faint bands at Vildbjerg. Small faint to moderate NLC in Finland at 62°N. Bands at Fort McMurray.
20/21	2110–2230	Bands in cloud gaps at Todmorden. Moderately bright display, all forms, by 7 observers in Finland.
21/22	2200–0030	Very faint bands visible through binoculars, Morpeth. Large bright display in N Finland.
22/23	2108–0045	Bands and billows in tropospheric cloud gaps in Orkney and Shetland. Bright and extensive display in Finland, all forms, dense brown–yellow structures described in eastern sky.
23/24 July	2130–0300	Very bright and extensive display, the best for many years, seen by 30 observers and meteorological stations throughout Britain on a clear night. NLC seen in cloud gaps in Finland. In Scotland large curved bands gave way to intensely bright whirls and knots near local midnight, then to strong billows high in NE towards dawn.
24/25		Billows up to 40° at Edmonton.
25/26	2100–2300	Small NLC at Kutunjärvi, Finland.
26/27	2100–2200	Faint bands and veil overhead at Todmorden. Bright NLC, all forms, observed throughout Finland and at Västerås, Sweden.
27/28	2045–2145	Faint veil suspected at Tampere but negative reports from several Finnish stations.
29/30	2130–2145	Doubtful. Possible small faint NLC at Kuopio but other Finnish stations negative. No NLC at Morpeth but faint band suspected at 2° at Swansea (Wales).
30/31	2000–2330	Faint display with bright individual structures, all forms, widely observed in Finland.
31 July/ 1 Aug.	2210–2245	Small faint NLC at Turku.
1/2	2315–0000	Bright, all forms, at Liminka, N Finland. Stations in S Finland negative.
2/3	2040–0300	Faint bands and billows in cloud gaps at Morpeth, suspect NLC in zenith at Todmorden. Small medium NLC in Finland.
3/4	2055–2300	Moderately bright bands and billows, S Finland.
4/5	2110–0050	Bands and billows, Orkney and Shetland; moderately bright bands, Kuopio and Illo, Finland.
7/8	2015–2330	Bright NLC, all forms, at Kuopio, Illo, Tampere and Joensuu. Described as fast-changing.
9/10	0010	Small medium NLC, veil and bands, at Kemiö, Finland.

Table II. *Nights in Finland and in Great Britain north of 54° N judged to have negative sightings of NLC*

Britain: May 8/9, 15/16, 21/22, 27/28; June 1/2, 3/4, 4/5, 7/8, 9/10, 11/12, 15/16; July 4/5, 9/10, 31/Aug. 1.

Finland: May 3/4, 4/5, 5/6, 6/7, 8/9, 9/10, 15/16, 31/June 1; June 9/10, 10/11, 11/12, 14/15, 15/16, 16/17, 17/18, 21/22, 25/26; July 2/3, 9/10, 13/14, 14/15, 18/19, 28/29; Aug. 6/7, 10/11, 14/15, 19/20, 25/26.

References

McConnell, D. 1987 Clouds of the twilight. *Astronomy*, **15**, 42–47.
Zwart, B. 1986 Lichtende nachtwolken. *Zenit*, **13**, 378–382.

551.553.8(420)

Exceptionally strong winds of 16 October 1987 over the south of England

Advisory Services Branch
Meteorological Office, Bracknell

Summary

A brief description is given of the exceptionally strong winds which occurred over the south of England on 16 October 1987.

On the evening of 15 October 1987 there was a depression with a central pressure of 972 mb in the vicinity of East Anglia. A front lying over the south of England linked this depression with another deep depression over the western entrance of the English Channel. To the north of the front there were cool, light to moderate north-easterly winds, whereas to the south there were stronger winds from the south-west.

By midnight the depression in the English Channel was centred over the south coast of Cornwall and had deepened to less than 958 mb. The associated front was moving quickly northward over the south of England and brought a band of heavy rain to the region. Behind the front there were strong winds with gusts of over 40 kn being reported over inland areas.

As the depression tracked north-eastwards into the North Sea the winds strengthened, with the strongest winds occurring over southern England between 0200 and 0600 GMT. Of particular note are the gusts of 80 kn or more between 0300 and 0500 GMT over the area south-east of a line from London to the Isle of Wight (see Fig. 1). By 0600 GMT a broad band of very strong winds covered most of

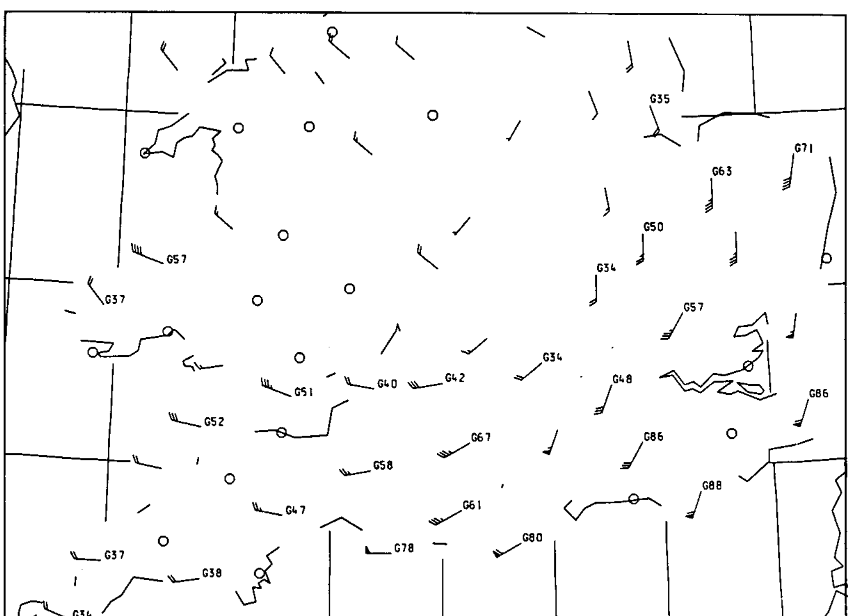

Figure 1. Mean wind speeds and gusts reported at 0500 GMT on 16 October 1987.

England south of a line from the Severn Estuary to the Wash, but by 0900 GMT the winds had decreased in strength over most areas except the north of East Anglia.

It is interesting to consider how unusual the winds were on 16 October 1987. Provided that sufficient long-term records are available from stations with sophisticated wind-recording equipment, it is possible by statistical methods to estimate the average interval in years between wind speeds of a given strength (the return period). However, it must be stressed that the return period is only an average interval so in reality extreme winds could occur more frequently. Table I gives the 19 sites with their highest mean speeds and/or gusts recorded on 16 October together with an indication of the approximate return period where available.

As yet the data have not been subjected to the usual careful scrutiny so the values quoted may be revised in the light of later examination.

Table I. *19 sites with their highest mean speeds and/or highest gusts recorded on 16 October 1987 between 0000 and 1300 GMT with an indication of the approximate return periods where available*

	Mean speed kn	Approximate return period years	Maximum gust kn	Approximate return period years
Brize Norton	25	Less than 10	50	Less than 10
Oxford Airport	35	Not available	62	Not available
Boscombe Down (Salisbury)	36	Less than 10	70	20
Hurn (Bournemouth)	37	10	62	10
Southampton	48	Not available	75	Not available
St Catherines (Isle of Wight)	58	Not available	90	Not available
Jersey	55	10	85	15
Herstmonceux (Eastbourne)	60	Not available	90	Not available
Langdon Bay (Dover)	62	Not available	90	Not available
Manston (Margate)	61	Over 500	86	Over 200
East Malling	37	Not available	74	Not available
Gravesend	34	Not available	74	Not available
Gatwick Airport	34	Less than 10	86	Over 300
London (Heathrow) Airport	39	20	66	40
London Weather Centre	44	200	82	120
Stansted Airport	34	10	65	20
Shoeburyness	55	Over 500	87	Over 500
Wattisham (Stowmarket)	48	45	72	10
Hemsby (Great Yarmouth)	45	Not available	78	Not available

In some areas the winds were not exceptional, having return periods of 20 years or less. However, in a few cases the return periods appear to be in excess of 200 years and possibly as long as 500 years in one or two cases. These figures suggest that in some areas the winds recorded on 16 October were exceptionally strong. Elsewhere in Britain, especially in western and coastal areas (and over mountains), such wind speeds occur much more frequently.

Review

Antarctic science, edited by D.W.H. Walton. 225 mm × 282 mm, pp. viii + 280, *illus.* Cambridge University Press, 1987. Price £25.00, US $39.50.

This book is a celebration and assessment of international co-operation since the signing of the Antarctic Treaty 25 years ago. After an introduction by Sir Vivian Fuchs, the first section concerns itself naturally with the history of the exploration, and there are some fine pictures of the sailing ships used in the rugged surroundings and descriptions of the toll these surroundings took. One may learn that Captain Cook was unimpressed with Antarctica and prophesied that it would be of no use – an early forecast gone astray! Also, it is rather worrying to think that no less a person than Gauss had miscalculated the magnetic South Pole by several hundred miles.

Subsequently there are sections on earth sciences, politics, biology and atmospheric science. Although I am a non-expert in all these subjects the authors are all experts from the British Antarctic Survey and they have all provided excellent text, bibliographies and index. There are many photographs, plenty in colour, and the diagrams are simple but instructive, reminiscent of Reihl's *Tropical Meteorology*. However, there are some rather gory photographs about whaling and one of a fish with its entrails hanging out with the distraught expression of one who has come round from the anaesthetic too early.

Some indication of the difficulty in observing the weather in the Antarctic can be gleaned from the fact that there were only 12 permanently manned weather stations in operation south of 55° S as late as 1955. However, the International Geophysical Year during 1957/58 made a considerable improvement.

Interestingly, there aren't any thunderstorms and hardly any rain in Antarctica, though fronds of ferns do appear on rocks (the result of a tropical climate many million years ago). The tectonic development of the area is described in chapter 13.

A fine bi-polar diagram of the earth's albedo reveals just how much of the surface is highly absorbent. Incidentally, the diagrams and photographs are unnumbered which leaves them less cluttered but makes the exact textual reference to them harder to find. This all leads on to space exploration and rocketry and a picture (novel to me) of an X-ray aurora from a satellite.

Looking to the way the future of exploration will unfold, chapter 18 contains the idea of science used as a tool for political defusion. The Antarctic Treaty is printed out in Appendix I, a useful reminder, and the whole book is written in non-technical terms as far as possible (not an equation in sight). Priced at £25, it sounds a lot to anyone over 50 years old, but there's plenty in it for many people, not only Antarctic buffs, and it is an excellent broadening-of-knowledge experience for anyone.

S.H. Barker

Books received

The listing of books under this heading does not preclude a review in the Meteorological Magazine at a later date.

Weather radar and flood forecasting, edited by V.K. Collinge and C. Kirby (Chichester, New York, Brisbane, Toronto, Singapore, John Wiley and Sons, 1987. £39.00) is based on a symposium held in the University of Lancaster, and examines the capabilities of weather radar with emphasis on operational experience in the United Kingdom. Hydrological aspects of flood forecasting, with specific real-time problems, are also discussed.

Satellite photograph — 2 September 1987 at 1550 GMT

This NOAA-9 visible image shows the cloud associated with a north-eastward moving Atlantic depression, with a central pressure of 973 mb. The cloud structure associated with the frontal zone is particularly well illustrated, due mainly to the general absence of an upper-cloud shield. South of 57° N, the front may be inferred to be a classical cold front with rearward-sloping ascent* since dense low and medium cloud terminates at a sharp forward boundary (close to the position of the surface cold front), whilst semi-transparent cirrus (where present) marks a sharp rearward boundary.

North and west of 57° N, where the front is probably occluded, a zone of low-level layered cloud, with embedded convection (as suggested by the 'lumpy' texture) terminates at a sharp rear edge. Cirrus, where present, lies within the forward portion of the front, with anticyclonically curved filaments defining a 'saw tooth' appearance to the forward limit of the cloud. This structure is characteristc of a split front where, due to forward-sloping ascent*, the front at upper levels (marked by the termination of upper cloud) has advanced ahead of that at lower levels (marked by the rearward edge of the lower cloud).

Within the circulation of the depression, extensive open cellular convection is present, except immediately behind the front where cloud formation is probably suppressed due to post-frontal subsidence.

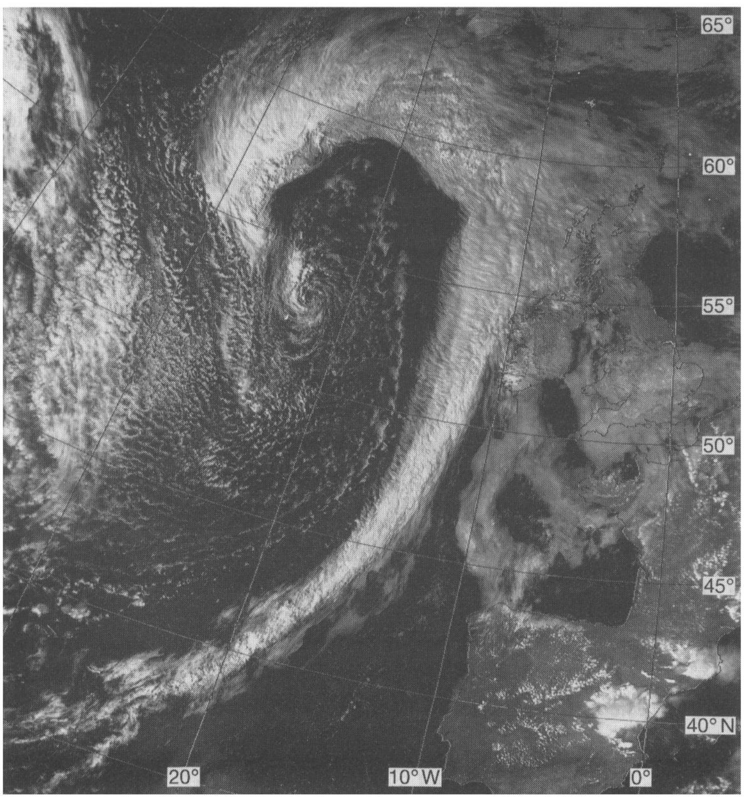

Photograph by courtesy of University of Dundee

* Browning, K.A.; Conceptual models of precipitation systems. *Meteorol Mag*, **114**, 1985, 293–319.

Meteorological Magazine

GUIDE TO AUTHORS

Content

Articles on all aspects of meteorology are welcomed, particularly those which describe the results of research in applied meteorology or the development of practical forecasting techniques.

Preparation and submission of articles

Articles for publication and all other communications for the Editor should be addressed to the Director-General, Meteorological Office, London Road, Bracknell, Berkshire RG12 2SZ and marked 'For *Meteorological Magazine*'.

Articles, which must be in English, should be typed, double-spaced with wide margins, on one side only of A4-size paper. Tables, references and figure captions should be typed separately.

Spelling should conform to the preferred spelling in the *Concise Oxford Dictionary*.

References should be made using the Harvard system (author, date) and full details should be given at the end of the text. If a document referred to is unpublished, details must be given of the library where it may be seen. Documents which are not available to enquirers must not be referred to.

Tables should be numbered using roman numerals and provided with headings. We consider vertical and horizontal rules to be unnecessary in a well-designed table; spaces should be used instead.

Mathematical notation should be written with extreme care. Particular care should be taken to differentiate between Greek letters and Roman letters for which they could be mistaken. Double subscripts and superscripts should be avoided, as they are difficult to typeset and difficult to read. Keep notation as simple as possible; this makes typesetting quicker and therefore cheaper, and reduces the possibility of error. Further guidance is given in BS1991: Part 1: 1976 and *Quantities, Units and Symbols* published by the Royal Society.

Illustrations

Diagrams must be supplied either drawn to professional standards or drawn clearly, preferably in ink. They should be about 1½ to 3 times the final printed size and should not contain any unnecessary or irrelevant details. Any symbols and lettering must be large enough to remain legible after reduction. Explanatory text should not appear on the diagram itself but in the caption. Captions should be typed on a separate sheet of paper and should, as far as possible, explain the meanings of the diagrams without the reader having to refer to the text.

Sharp monochrome photographs on glossy paper are preferred: colour prints are acceptable but the use of colour within the magazine is at the Editor's discretion. In either case contrast should be sufficient to ensure satisfactory reproduction.

Units

SI units, or units approved by WMO, should be used.

Copyright

Authors wishing to retain copyright for themselves or for their sponsors should inform the Editor when they submit contributions which will otherwise become UK Crown copyright by right of first publication.

It is the responsibility of authors to obtain clearance for any copyright material they wish to use before submitting it for publication.

Free copies

Three free copies of the magazine are provided for authors of articles published in it. Separate offprints for each article are not provided.

Meteorological Magazine

December 1987

Vol. 116
No. 1385

CONTENTS

Contributions: it is requested that all communications to the Editor and books for review be addressed to the Director-General, Meteorological Office, London Road, Bracknell, Berkshire RG12 2SZ, and marked 'For *Meteorological Magazine*'. Contributors are asked to comply with the guidelines given in the *Guide to authors* which appears on the inside back cover. The responsibility for facts and opinions expressed in the signed articles and letters published in *Meteorological Magazine* rests with their respective authors. Authors wishing to retain copyright for themselves or for their sponsors should inform the Editor when submitting contributions which will otherwise become UK Crown copyright by right of first publication.

Subscriptions: Annual subscription £27.00 including postage; individual copies £2.30 including postage. Applications for postal subscriptions should be made to HMSO, PO Box 276, London SW8 5DT; subscription enquiries 01–211 8667.

Back numbers: Full-size reprints of Vols 1–75 (1866–1940) are available from Johnson Reprint Co. Ltd, 24–28 Oval Road, London NW1 7DX. Complete volumes of *Meteorological Magazine* commencing with volume 54 are available on microfilm from University Microfilms International, 18 Bedford Row, London WC1R 4EJ. Information on microfiche issues is available from Kraus Microfiche, Rte 100, Milwood, NY 10546, USA.

ISBN 0 11 727976 5

ISSN 0026–1149

Printed for HER MAJESTY'S STATIONERY OFFICE
Dd 240020 C14 11/87